The smarter, the stronger: Intelligence level correlates with brain resilience to systematic insults

(Article begins on next page)

Accepted Manuscript

The Smarter, the Stronger: Intelligence Level Correlates With Brain Resilience To Systematic Insults

Emiliano Santarnecchi , Simone Rossi , Alessandro Rossi

Please cite this article as: Santarnecchi E, Rossi S, Rossi A, The Smarter, the Stronger: Intelligence Level Correlates With Brain Resilience To Systematic Insults, *CORTEX* (2015), doi: 10.1016/ j.cortex.2014.11.005.

The Smarter, the Stronger: Intelligence Level Correlates With Brain Resilience To Systematic Insults

Emiliano Santarnecchi[1-2]*,Simone Rossi[1], Alessandro Rossi[1]

[1] Department of Medicine, Surgery and Neuroscience, Neurology and Clinical Neurophysiology Section, Brain Investigation & Neuromodulation Lab, University of Siena, Italy

[2] Berenson-Allen Center for Non-Invasive Brain Stimulation, Beth Israel Medical Center, Harvard Medical School, Boston, MA, USA

Running title: Intelligence and brain resilience

Words count: Abstract 182, Legends 998, Introduction 736, Discussion 2339

Figures: 6 figures; 6 supplemental figures.

Tables:1

Financial disclosures: All authors report no conflict of interest.

*Corresponding author:

Emiliano Santarnecchi

Policlinico "Le Scotte", Viale Bracci, 2,

Brain Investigation &Neuromodulation Lab., University of Siena, Italy

Siena, 53100, Italy

esantarn@bidmc.harvard.edu

mobile: (ITA) +39.3382149984; (US) +1 (781) 298-1072

fax: +39.0577270260

1

Abstract

Neuroimaging evidences posit human intelligence as tightly coupled with several structural and functional brain properties, also suggesting its potential protective role against aging and neurodegenerative conditions. However, whether higher-order cognition might in fact lead to a more resilient brain has not been quantitatively demonstrated yet. Here we document a relationship between individual intelligence quotient (IQ) and brain resilience to targeted and random attacks, as measured through resting-state fMRI graph-theoretical analysis in 102 healthy individuals. In this modeling context, enhanced brain robustness to targeted attacks in individuals with higher IQ is supported by an increased distributed processing capacity despite the systematic loss of the most important node(s) of the system. Moreover, brain resilience in individuals with higher IQ is supported by a set of neocortical regions mainly belonging to language and memory processing network(s), whereas regions related to emotional processing are mostly responsible for lower IQ individuals. Results suggest intelligence level among the predictors of post-lesional or neurodegenerative recovery, also promoting the evolutionary role of higher order cognition, and simultaneously suggesting a new framework for brain stimulation interventions aimed at counteract brain deterioration over time.

Highlights

- Intelligence quotient correlates with brain resilience to targeted and random attacks

- Language and memory-related regions are strongly related to brain resilience and IQ

- Regions related to emotion processing are crucial for resilience in Low-IQ subjects

1.0 Introduction

Intelligent people live longer (Deary 2008). The initial surprise about such a linear relationship between intelligence and life expectancy/mortality has been replaced byseveral evidences confirming that health inequality partly depends by the individual intelligence level (Batty et al. 2009;Batty, Shipley, Gale, Mortensen, and Deary 2008). Several factors might account for this interaction, such as the association between early-life intelligence and higher levels of education/professional occupations, or the tendency to pursue in more healthy habits in terms of sports, smoking, dietary regime and weight control. Furthermore, the correlation between intelligence quotient (IQ) and mortality has been also considered a reductive argumentation respect to a broader biological theory suggesting its relationship with the "overallsystem integrity", thus implying a "more intelligent" brain to be associated to a likewise well-functioning body, thereby increasing the probability of a longer life (Deary 2008;Deary and Der 2005).

On the other side, in the last decade the concept of cognitive reserve (CR) has been introduced (Stern 2009a;Stern 2009b), as a framework specifically addressing the individual variability between expected and actually observed cognitive capacities across pathological brain conditions like cerebrovascular disease (Murray et al. 2011), Parkinson's disease (Poletti, Emre, and Bonuccelli 2011) and multiple sclerosis (Langdon 2011), as well as in healthy elderly subjects with brain atrophy (Stern 2002;Stern 2009b). Interestingly, the CR model mainly concerns higher-order cognitive functions which pertain to the general intelligence factor "*g*", hence promoting the idea of intelligence as a "buffer"helping to assure a more favorable disease outcome in case of brain pathology (Satz, Cole, Hardy, and Rassovsky 2011).

4

Despite the amount of data sustaining the CR model, whether intelligence should be considered just as a tool to indirectly achieve a longer life expectancy, or it must be conceptualized as a functionally relevant phenotype -that is, expression of a cognitively optimized brain towards ageing itself or intercurring neurological insults- is still a matter of debate. Consequently, the current study is aimed at investigate the hypothesis that a higher IQ translates into a functionally more resilient brain towards physiological aging or pathology-related loss of regional efficiency, defining "robustness" in the context of a graph-topological analysis already used to characterize complex networks behavior at several biological levels (Albert, Jeong, and Barabasi 2000a).

Recent neuroimaging evidence has suggested how the human brain is a complex system of interconnected regions spontaneously organized into distinct networks (Achard and Bullmore 2007a;Craddock et al. 2013;Fox, Snyder, Vincent, Corbetta, Van Essen, and Raichle 2005;Hagmann et al. 2008;Shehzad et al. 2014;Sporns, Tononi, and Edelman 2002), with such organization being highly correlated with individual differences in manifest behaviour, also including complex phenotypes like intelligence (Santarnecchi, Galli, Polizzotto, Rossi, and Rossi 2014;van den Heuvel, Stam, Kahn, and Hulshoff Pol 2009). Moreover, brain modeling based on graph-theory allowed to describe such complex organization using indexes referring to notable complex networks properties (Sporns 2014), like their capacity for simultaneous local and distributed information processing (Eguiluz, Chialvo, Cecchi, Baliki, and Apkarian 2005;Sepulcre, Liu, Talukdar, Martincorena, Yeo, and Buckner 2010), their organization into separate but integrated modules (Achard and Bullmore 2007a;Sporns 2013),and their power-law distribution of network nodes importance (Achard, Salvador, Whitcher, Suckling, and Bullmore 2006). Notably, this topological organization, shared by several complex biological systems,

often corresponds to an increased "robustness" (or resilience) against system failure (i.e. random error) or deliberated lesioning procedures (targeted attacks) (Albert, Jeong, and Barabasi 2000b;Bak and Paczuski 1995;Kitano 2004). By providing an estimation of the residual network functionality after complete or partial lesions, network simulations allow to infer the response of a complex system to both random or targeted attacks, thereby allowing a quantification of complex networks' "goodness" and of their rate of survival against unexpected system malfunctioning. Assuming such network robustness as a "dominant" trait, whether intelligence is associated with such trait is an unexplored argument of absolute interest, including possible implications as to the evolutionary role of human higher order cognition.

We therefore estimated brain functional robustness towards both random error (RE) and targeted attacks (TA) in a group of 102 healthy subjects (49 males, average age = 34 yrs, SD = 14, range 20-60), in the attempt to address the following issues: (i) does a higher intelligence profile level correspond to a more robust brain? If so, (ii) which are the brain regions more or less susceptible to TA or RE? (iii) Given the different neurobiological meaning of RE and TA,is there a specific relationship between intelligence and these two brain robustness indexes? Finally, (iv) given the theoretical yet practical differences between crystallized (Gc) and fluid intelligence (Gf) abilities -respectively representing education-related and more innate "on the spot" cognitive abilities (Nisbett et al. 2012) - do both equally contribute/correspond to such robustness?

2.0 Materials and Methods

Specific details about the cognitive measures and fMRI preprocessing are included as supplemental material and methods. The following sections cover the details about brain resilience computation including networks definition, lesioning process and statistical analysis.

2.1 Sample and behavioral measures

Behavioral and neuroimaging data are part of the freely-available NKI-Rockland database, belonging to the FCP/INDI sharing initiative (www.fcon_1000.projects.nitrc.org), including a phenotypic characterization of 207 healthy subjects (age range 4 to 85 years), as well as structural (anatomical and Diffusion Tensor Imaging - DTI) and functional (resting-state fMRI) neuroimaging data. Considering our aim to characterize a possible link between individual brain robustness and intellectual level, a first concern has been to avoid conditions where an additional modulation of these two factors might be present. Thus, we decided to circumscribe our analysis to adult subjects (20>sample<60 years), limiting the effect of developmental and ageing-related changes of both cognitive and cerebral architecture. A further selection of subjects was performed to ensure *(i)* an equal number of males and females, given the evidence of interactions between gender and intellectual abilities (Haier, Jung, Yeo, Head, and Alkire 2005;Payton 2009), *(ii)* an equal distribution of age groups (decades) within the overall group and *(iii)* that all subjects were right-handed. The selection resulted in a final sample of 102 right-handed subjects (49 males), with mean age of 34 years (range 18-60, SD = 14) and available IQ scores representing overall (Full-scale) IQ as well as verbal and visuospatial IQ scores, respectively considered as indexes of Gc and Gf.

2.2.1 Network lesioning procedure

Network nodes were defined by parcellating the brain into 90 cortical and subcortical ROIs according to the Automatic Anatomical Labeling atlas (AAL) (Tzourio-Mazoyer et al. 2002), one of the most commonly employed atlas for network analyses (Achard and Bullmore 2007a;Achard, Salvador, Whitcher, Suckling, and Bullmore 2006;Liu et al. 2008;Wang, Li, Metzak, He, and Woodward 2010). Details about thresholding and sparsity have been included in the supplemental methods section. For the sake of readability, all the fMRI preprocessing, networks definition and thresholding, graph theoretical metrices computation and lesioning procedures are schematized in Fig.1.

As suggested in the introduction, robustness estimation comprehended two approaches for network lesioning, based on random or targeted node removal. These procedures involve the calculation of several topology indices, both for guiding the depletion process itself and for the estimation of network "well-being" after each depletion, whose explanation requires to assume: (N) as the set of all nodes in the network, (n) as the number of nodes, (k) as a specific node, (L) as the set of all links in the network, (l) as the number of links, (i, j) as the link between nodes i and j, (aij) as the connection status between i and j (aij=1 when link i, j exists; aij = 0 otherwise). All the graph properties have been calculated using Matlab functions included in the Brain Connectivity Toolbox (https://sites.google.com/site/bctnet/). As suggested in the previous section, individual functional connectivity matrices have been thresholded by selecting a progressively larger portion of all possible brain connections, leading to the creation of one hundred different sparsity matrices for each subject. Considering that each lesioning simulation comprised 90 depletions (see Fig.1B), and that it has been performed on each sparsity matrix, the overall lesioning process resulted in 90 [depletions] * 100 [sparsity matrices] * 102 [participants] simulations, separately for TA and RE.

2.2.2 Targeted Attacks and Random Errors

The purpose of targeted attacks (TA) procedure is to test the specific importance of certain network nodes for overall network stability. Usually, nodes removal follows a specific order which reflect the nodal properties of interest, for instance its importance for distributed information processing, local computation or modularity of the system. Previous studies about brain robustness have focused on different nodal properties, suggesting "centrality" measures as those providing the best robustness estimation (Alstott, Breakspear, Hagmann, Cammoun, and Sporns 2009). Well-known measures of centrality are the *(i)* degree, *D*, and the *(ii)* betweness centrality, *Bc*: while the *D* of a node k is the number of edges connecting it to other nodes, so that largely connected nodes show higher degrees, *Bc* is expression of the number of shortest node-to-node paths that pass through a specific node k, indicating how such node takes part into overall brain information processing by supporting other nodes communication through fast (i.e. short) connections. Even though there are evidences suggesting *Bc* as the best estimate of centrality for network robustness simulation (Alstott, Breakspear, Hagmann, Cammoun, and Sporns 2009), we also computed the results defining the target nodes by using two additional criteria, i.e. the nodal degree and strength of functional connectivity. Results obtained using these indexes are reported in figure S6. Therefore, *Bc* for the node i has been defined as:

$$bc_i = \frac{1}{(n-1)(n-2)} \sum_{\substack{h,j \in N \\ h \neq j, h \neq i, j \neq i}} \frac{\rho_{hj}(i)}{\rho_{hj}'}$$

where ρ_{hj} is the number of shortest paths between h and j, and ρ_{hj} (i) is the number of shortest paths between h and j that pass through i. As shown in Fig1.B, the lesioning process consisted in the *(i)* estimation of centrality values for each node of the AAL atlas (say *Bc*), *(ii)* sorting of

9

nodes based on their *Bc* value, *(iii)* removal of the node with higher *Bc* value. This process is recursively applied since all the nodes have been deleted, leading to the progressive creation of 90 matrices (one for each AAL atlas region).

Differently, random errors (RE) are thought to simulate a completely different phenomenon, which may affect complex network, i.e. the occurrence of a system failure. Random in nature, this event may cause or not a severe impairment to system integrity depending on which nodes is being involved. RE are conducted by *(i)* creating a 1*90 vector of randomly selected regions, and by lesioning the network by cutting the node corresponding to position (1,1) in the vector. A new 1*89 random vector (containing all regions except for the already cut node) is then created and the process continues till all nodes have been removed. To ensure a more reliable estimation we performed the entire process 100 times for each matrix and averaged the resulting robustness estimates.

Theoretically, the intrinsic structure of complex networks following a power-law degree distribution, like the human brain, guarantees an higher protection towards RE, by concentrating the very large part of information processing on a limited number of core regions which, in terms of probability, are supposed to be more difficult to be affected by a random attack. On the other side, TA are thought to be more effective in networks following such distribution, with even a few surgically planned resections capable to generate highly significant network impairment.

2.2.4 Network integrity against attack

Before the overall process, and between each node(s) depletion, several indices of network integrity are calculated, so that a "time course" of brain robustness is obtained while all atlas regions are progressively removed. This allows to caught a drop into robustness level at a

certain point along the process, which corresponds to the specific removal of a single or a small set of brain regions. We calculated measures describing both integration and segregation of functions within the brain, aiming at caughting the impact of network lesioning on *(i)* distributed and *(ii)* local processing. Regards *distributed processing*, two indices were computed, namely the Largest Connected Component –*LCC* and the Global efficiency – *E*. The *LCC* is the typical index usually applied for complex networks robustness estimation (Albert, Jeong, and Barabasi 2000b;Alstott, Breakspear, Hagmann, Cammoun, and Sporns 2009). Basically, it reflects the overall network "connectedness", that is the rate at which is possible to directly or indirectly connect each node in the network to each other. Perfectly connected networks, where all nodes are linked to each other forming a unique *component*, naturally guarantee a higher level of information spreading. However, complex network usually show a subset of nodes which play a crucial role for maintaining the network "connected", so that their depletion cause most severe damage to the overall network integrity by making a large number of other nodes "unreachable", i.e. disconnected from the component. Thus, *LCC* is defined as the largest number of nodes constituting a component after each depletion, and calculated through the estimation of a distance matrix - *d*, whose *ij* values represent the shortest path length (or distance) between all pairs of nodes, computed as:

$$d_{ij} = \sum_{a_{uv} \in g_{i \longleftrightarrow j}} a_{uv'}$$

with $g_{i \leftrightarrow j}$ representing the shortest path between nodes i and j (disconneted pairs=∞). Each cell within the resulting matrices represents the minimum number of steps (node-to-node connections) required to connect each pairs of nodes, so that a (i,j) blank cell indicates the

11

impossibility to directly or indirectly connect node i and j. Consequently, higher *LCC* values represent higher levels of connectedness.

Network *E* is defined as:

$$E = \frac{1}{n} \sum_{i \in N} E_i = \frac{1}{n} \sum_{i \in N} \frac{\sum_{j \in N, j \neq i} d_{ij}^{-1}}{n-1},$$

At a neurophysiological level, high *E* network is guaranteed by nodes placed at short distances from each other, a configuration which enables them to interact more directly, i.e. faster, consequently promoting high functional integration. In this context, higher values of *E* represent better overall brain information processing. Despite one of the most used network integration measures is the average path length, representing the average number of steps along the shortest paths for all possible pairs of network nodes, here we preferred *E* because of its lower sensitivity to the presence of disconnected or very weakly connected nodes (Bullmore and Bassett 2011;Sporns and Zwi 2004).

Differently, *local processing* is expression of adjacent neuronal population synchronization, a functional prerequisite for several cognitive functions within the motor, visual, somatosensory and also memory domains (Sepulcre, Liu, Talukdar, Martincorena, Yeo, and Buckner 2010). Here we characterized brain segregation using the Local efficiency index – E_{Loc}, a measure of the average efficiency within local subgraphs or neighborhood. E_{Loc} has been calculated as follow:

$$E_{loc} = \frac{1}{n} \sum_{i \in N} E_{loc,i} = \frac{1}{n} \sum_{i \in N} \frac{\sum_{j,h \in N, j \neq i} a_{ij} a_{ih} [d_{jh}(N_i)]^{-1}}{k_i(k_i - 1)}$$

12

where$E$loc,i is the local efficiency of node i, and $djh(Ni)$ is the length of the shortest path between j and h, that contains only neighbors of i. Higher level of E_{Loc} represent better information processing at local level.

Furthermore, other topological indexes have been computed in order to determine the individual small-worldness window (SW) where the robustness indexes have been extracted. First of all, SW has been calculated as:

$$S = \frac{CC \, / \, CC_{rand}}{L \, / \, L_{rand}}$$

where CC-CC_{rand} and L-L_{rand} respectively represent the clustering coefficients (CC) and the characteristic path lengths (L) of the actual network and of a random network ($_{rand}$). The *average path length*, L, is defined as:

$$L = \frac{1}{n}\sum_{i \in N} L_i = \frac{1}{n}\sum_{i \in N} \frac{\sum_{j \in N, j \neq i} dij}{n-1}$$

where Li is the average distance between node i and all other nodes. It represents the average number of steps along the shortest paths for all possible pairs of network nodes. As an index of information processing efficiency, shorter L values usually stand for more efficient networks. The *clustering coefficient*, CC, is defined as:

$$CC = \frac{1}{n}\sum_{i \in N} CC_i = \frac{1}{n}\sum_{i \in N} \frac{2t_i}{k_i(k_i-1)}$$

whereCC_i is the clustering coefficient of node i (CC_i=0 for k_i<2). CC is expression of each node's tendency to cluster with neighboring nodes and is thus considered a reliable index of network local connectivity. The individual SW window was composed by those matrices showing a Small-world value > 1 (Humphries and Gurney, 2008). Compatible with what

13

previously reported, our sample shows network densities corresponding to SW ranging, on average, from 10 to 31% (Fig.2B).

2.3 Statistical analysis

Statistical analyses were carried out over all topological measures (LCC, E, E_{Loc}, Bc), even though the main outcome of interest was composed by LCC as a direct expression of brain integrity after each node removal (Alstott, Breakspear, Hagmann, Cammoun, and Sporns 2009). We first conducted a linear regression analysis to assess the relationship between IQs (FSIQ, VIQ, PIQ) and the average topological properties of all the matrices corresponding to the small-worldness window of each subject (Humphries and Gurney 2008). Average values for each network property (LCC, E, E_{Loc}, Bc) have been inserted as independent variables, while IQs scores have been separately included as dependent variables. Furthermore, given the results of regression analysis, an Analysis of Covariance (ANCOVA) specifically contrasting the LCC values of High and Low-IQ subjects within the small-world window was computed, including age, Body Mass Index (BMI), total brain volume (TBV) and gender as covariates. An alpha=.05 was chosen as significance level for all the analyses, post-hoc comparisons have been computed using Bonferroni correction (p<.05).

The ANOVA has been also used in order to verify the existence of significant between-groups differences in the distribution of LCC values as a function of age and intelligence. LCC values computed within the small-world window have been thus inserted as dependent variables, with Group (High and Low-IQ) and Decades as independent variables. Specifically for this analysis, a subgroup of subjects belonging to the 61-70yrs decade has been included in the sample, resulting in 5 decades (21-30yrs, 31-40yrs, 41-50yrs, 51-60yrs, 61-70yrs). Moreover,

14

given an *a priori* knowledge about a potential role for brain weak connections into discriminate subjects with High and Low IQ (Santarnecchi, Galli, Polizzotto, Rossi, and Rossi 2014a), topological measures and robustness indexes have been also computed outside the SW window, that is along the entire sparsity range (1%-100%). The same regression model has been than calculated by including progressively weaker connectivities (1% sparsity steps), looking for potential interactions between intelligence and robustness values derived from connectivity matrices including strong, other than weak connections.

2.4 Definition of robustness-related brain regions

Along with the identification of an intelligence-brain robustness interaction, we also aimed at identifying the importance of specific anatomical regions for the maintaining of brain integrity. Consequently, we performed a multivariate classification procedure to assess the contribution of each AAL atlas region to the significant difference in brain robustness to TA observed between High and Low-IQ groups. Assuming the *LCC* as the primary index of interest, a vector of the drop in *LCC* size after each region removal has been created (focusing on individual SW windows) for each subject, resulting in a 102x90 matrix. Using Weka software (Frank, Hall, Trigg, Holmes, and Witten 2004), a support vector machine (SVM) algorithm was tested through leave-one-out cross-validation (folds = 101), resulting in an estimation of the overall correct classification percentage (Sensitivity, Specificity, area under the ROC curve) as well as to a node specific discriminative weight as expression of each region contribution to the overall classification process. However, as the pattern obtained through SVM classification is multivariate, regions above the 95th percentile and below the 5th percentile have been assumed as representing, respectively, brain regions more sensitive to the lesioning process in the High and Low-IQ groups - that is those regions whose removal strongly affect brain integrity by

significantly decrease the size of the *LCC* (Santarnecchi, Galli, Polizzotto, Rossi, and Rossi 2014). Images were plotted on an inflated three-dimensional brain (Fig.3), with this graphical representation showing only the regions that carry most of the discriminative weight - that is, those relatively more important to forming the decision boundary.

Furthermore, the identification of the most important regions for the observed intelligence-robustness interaction allows for the investigation of node-specific features supporting such relationship. Therefore, both *(i)* pairwise functional connectivity and *(ii)* seed-to-networks analyses have been computed for all the aforementioned regions. Briefly, functional connectivity has been computed -at the single subject level- as the Pearson correlation coefficient between the time series of all the regions included in the AAL atlas. Differences in the average pattern of connectivity at the group level (High *vs* Low-IQ) have been calculated using a False Discovery Rate (p.=0.05) correction, highlighting increase and decrease in the strength of specific connections between each region and the rest of the brain.

At the network level, the average time course of BOLD fluctuations within specific resting state networks (RSNs) of interest have been extracted, thus representing the average connectivity pattern of such networks in individuals with High and Low-IQ scores. Consequently, correlation values between RSNs time courses and those of the most discriminant regions have been compared across groups (p.<0.05, Bonferroni corrected), highlighting specific intelligence-related relationship between such regions and specific networks. RSNs have been defined as the results of previous investigations (Allen et al. 2011a;Mantini, Perrucci, Del, Romani, and Corbetta 2007), resulting in the definition of nine well-known networks: default-mode, fronto-parietal control, frontal attention, language, somatomotor, auditor, visual and (right-left) working memory networks.

16

3.0 Results

A synthetic scheme of the overall procedure for functional connectivity estimation and network lesioning is reported in Figure 1. It is noteworthy that, given the limitation of available neuroimaging database in terms of sample size and thus age distribution per decade, our approach is aimed at identifying a relationship between intelligence and brain resilience regardless of age, therefore all analyses have been computed including age as a covariate. However, given the potentially relevant role of age for future investigations about brain robustness, an additional exploratory analysis of the age*intelligence*robustness interaction has been completed on the available data and included as part of the supplementary materials. Moreover, in order to rule out the role of brain reserve in such relationship, individual total brain volume was regressed out from the analysis as well. Additional details about data preprocessing and network analysis are included in the experimental procedures section and supplemental information.

3.1 Correlation between intelligence and brain resilience

Significant correlations between brain robustness and Full Scale, Verbal and Performance IQ scores emerged (Fig.2A). Even though these correlations were present for both resilience indexes and all IQ scores, a pattern of significantly stronger correlation betweenthe robustness towards TA -expressed as the size of the largest connected component (*LCC*) (Albert, Jeong, and Barabasi 2000b)- and FSIQ [$r_{(101)}$ =.75, p<.001, R^2=.57], VIQ [$r_{(101)}$ =.70, p<.01, R^2=.50]and PIQ [$r_{(101)}$ = .53, p<.01, R^2=.26]respect to the impact of RE [FSIQ, $r_{(101)}$ =.45, p<.001 , R^2=.12; VIQ, $r_{(101)}$ = .47, p<.01, R^2=.14; PIQ, $r_{(101)}$ = .41, p<.01, R^2=.15] emerged (results for other indexes of distributed and local information processing are included as Supplemental Results). The

computation of brain robustness as a function of network sparsity allowed addressing potential differences in the size of the *LCC* across network densities, and thus to evaluate the impact of such network thresholding-dependent procedure on robustness estimation. As previously reported (Achard and Bullmore 2007a;Watts and Strogatz 1998;Wu et al. 2013), valid arguments sustain the *a-priori* computation of network topology (and robustness) within specific network density windows, mainly focusing on brain properties obtained by looking at network configurations resembling the so-called small-world (SW) topological organization (Figure 2B) (Achard and Bullmore 2007b). Therefore, the results of statistical models computed within the SW window have been considered the main outcome of interest. However, TA and RE simulations produced strongly different estimation of brain robustness in respect to the percentage of nodes that were included in the network (Fig. 2B). Accordingly, panel C highlights how the intensity of the correlation with intelligence scores fluctuates as a function of network sparsity, with potential opposite results for TA when weak brain connections are taken into account (sparsity 80-100%). Results related to other network topological properties are included as supplemental results.

3.2 Identification of resilience-related brain regions

By investigating the topological features responsible for the observed intelligence-related difference in robustness towards TA, we focused on the identification of those regions whose exclusion from the network lead to the larger loss of brain robustness. Therefore, by applying a median split segmentation of the entire sample we obtained two groups representing participants with High (n = 57; mean age = 35±12; mean FSIQ = 119±7) and Low (n = 45; mean age = 36±10; mean FSIQ = 84±5) IQ levels (Table 1), with no differences for age (t=.345, *p*=.534) and

gender distribution (χ^2 =.403, p=.546). The analysis of the regions mostly responsible for the intelligence-robustness interaction was carried out by means of a support vector machine (SVM) classification procedure, leading to a IQ-groups classification accuracy of 82,7% (CI=.645-.876;Sensitivity=.712; Specificity=.867; AUC .912). The distribution of the differences in the average *LCC* drop for each single region of the AAL atlas used to inform the SVM algorithm is included in FigureS3. Control analysis using SVM on those regions identified as the most important into separating High and Low IQ participants (12/90) led to an IQ-group classification accuracy of 75,3% (CI=.612-.798; Sensitivity=.689; Specificity=.833; AUC .856). Among High-IQ subjects, these regions mostly belonged to a bilateral network encompassing regions anatomically and functionally crucial for language processing and production, like pars-opercularis of the inferior frontal gyrus (BA44) and the middle frontal gyrus (BA46), which basically compose the Broca's area, and the inferior parietal lobe (BA40), mostly corresponding to Wernike's region along with the supramarginal gyrus and a portion of middle temporal gyrus (Fig.3A) (Binder, Frost, Hammeke, Cox, Rao, and Prieto 1997a;Cappa 2012;Papathanassiou, Etard, Mellet, Zago, Mazoyer, and Tzourio-Mazoyer 2000;Simos et al. 1999). Moreover, regions associated to memory processing (mid and inferior temporal lobe [BA21, BA20], middle frontal gyrus [BA46], posterior cingulate cortex [BA23]) have been also identified. Interestingly, regions being crucial for brain integrity in Low-IQ subjects were all, partially or completely, related to the manipulation of emotional content, more precisely left amygdala, right anterior cingulated cortex (ACC) and left temporal pole (Devinsky, Morrell, and Vogt 1995;Jimura, Konishi, and Miyashita 2009;Kobayashi 2011;Morris et al. 1998)(Fig.3B).

Given such language-related difference, the possibility of a gender-related effect was investigated, resulting in a null difference in the robustness level between female and male

participants (Fig.4A). Such finding promoted a further exploration of possible differences in the functional connectivity profile of these regions with respect to their correlation with intelligence and brain resilience to lesions. In the context of a generalized difference in the overall connectivity profile of High and Low IQ subjects (Fig.4B), we consequently investigated for potential differences in the average regional connectivity of subjects with High and Low IQs by the means of seed-based pairwise connectivity analysis. The results of between-group comparisons (p<.05, False Discovery Rate -FDR- corrected) for language network's nodes (additional regions' connectivity profiles are included in Figure S45) and emotion-related regions are reported in Figure 4C and Figure 5B respectively. Finally, in order to get an insight about the role of such regions in the overall brain organization at rest, we also looked at the connections between these regions and anatomically defined resting-state networks (RSN) (Fox, Snyder, Vincent, Corbetta, Van Essen, and Raichle 2005). Therefore, average seed-to-network functional connectivity values have been calculated in both groups, referring to well known RSN encompassing the default-mode, fronto-parietal control, frontal attention, language, somatomotor, auditor, visual and working memory networks (Allen et al. 2011b;Mantini, Perrucci, Del, Romani, and Corbetta 2007). The results of group comparison (all p<.05, Bonferroni corrected) are presented in Figure 4D (High>Low IQ)and Figure 5A (Low>High IQ) as the average seed-to-network profile of subjects with High and Low-IQ. Despite region-specific variations in the differential connectivity patterns, an overall trend for a major involvement of the fronto-parietal control, frontal attention and working memory RSNs emerged in both groups. Additional details about the aforementioned statistical analyses are included as supplementary Material and Methods.

Finally, given the interesting link between CR and age (Bastin et al. 2012;Zihl, Fink, Pargent, Ziegler, and Buhner 2014), we also looked at their potential interaction with intelligence. By contrasting a model including the average *LCC* values of High and Low-IQ subjects in different decades (see supplemental Methods and Results), we identifying a trending to significance interaction between robustness, age and intelligence, possibly forced by an augmented robustness in High-IQ subjects older than 50 years respect to Low-IQ ones, with data related to TA being more coherent along the entire age range (Fig. S4).

4.0 Discussion

Recent advances in brain modeling and neuroimaging techniques have contributed to a better understanding of the neurobiological correlates of intelligence (Haier, Jung, Yeo, Head, and Alkire 2004;Penke et al. 2012a;Penke et al. 2012b;van den Heuvel, Stam, Kahn, and Hulshoff Pol 2009). Interestingly, the correlation between intelligence and epidemiological factors has been demonstrated as well, with higher IQ people being reported as having, for instance,an higher survival rate and a better social economic status (Deary 2008;Gottfredson 2004;Pierce, Miller, Arden, and Gottfredson 2009). While intelligence level has been promoted as a mediator for more efficient behavior, like improved decision-making abilities in everyday life, no evidence has been reported for a more direct link between intelligence level and brain intrinsic properties related to its ability to cope with the loss of its functional units. Here we document a correlation between IQ and brain robustness as measured through resting-state fMRI graph-theoretical analysis, with specific subsets of cortical and subcortical regions mostly responsible for such brain feature. This suggests a possible link between the development of specific cognitive abilities, the consequential shaping of their neuroanatomical and

neurophysiological substrates, and a resultant behavioural pattern inherently leading to improved robustness towards brain insults.

Robustness is a ubiquitously observed property of complex, evolvable systems (Kitano 2004). Given its multidimensional nature, encompassing organic biology, mathematics, sociology and engineering, our finding allow for a series of theoretical and practical considerations. Therefore, we will summarize our discussion focusing on *(i)* the possible biological underpinnings of the intelligence-brain robustness interaction, *(ii)* its impact into determining individual robustness towards acute or chronic brain diseases, *(iii)* the investigation of the role of the specific regions responsible for the observed correlation and the meaning of the different interaction with TA and RE, as well *(iv)* the potential implications of these results concerning Non-Invasive Brain Stimulation (NiBS) techniques.

4.1 Robustness and evolvability

Looking at the evolutionary role of "robustness" for biological system, a correlation between intelligence and brain robustness to damage sounds like an oversimplified yet expected finding. While conceptualized within the framework of different self-organization models, like the "Highly Optimized Tolerance" (HOT) (Carlson and Doyle 1999), the scale-free network by preferential attachment (Barabasi and Albert 1999) and the self-organized criticality ones (Bak and Paczuski 1995), robustness is generally defined as the main feature that allows a system to maintain its functions in case of external and internal perturbations (Kitano 2004). It indeed represents a clear example of those fundamental systems-level phenomena, self-emerging from the inherent structure of the system itself and impossible to be fully understood by looking at the individual components of the network. Interestingly, from the biological point of view, robustness usually shares the same architectural requirements of evolvability, giving reason why

it is ubiquitously reported in living organisms that have evolved (Kitano 2004). More generally, two central features of complex systems' architecture have been proposed as able to facilitate evolvability and robustness: a highly resilient and conserved core of processes working as an interface for diverse inputs and outputs (signaling, nutrients and products at the molecular biology level), and a more versatile mechanism, known as "weak linkage", that somehow sustains and facilitate the proper exchange of information between different units of the main core (de Visser et al. 2003;Kirschner and Gerhart 1998). Interestingly, the human brain is considered among the most complex system in nature, with some of its structural features strongly resembling network behaviors ascribed to other biological systems, for instance small-world configuration (Achard and Bullmore 2007b;Downes et al. 2012). Furthermore, the very idea of a stable "central core" has been recently translated at the brain level as well, with a "functional backbone" documented as the main component of resting and evoked activity in human and other mammals brains (van den Heuvel, Kahn, Goni, and Sporns 2012;van den Heuvel and Sporns 2013). As a complementary finding, in a previous study we have documented how the vast majority of intelligence-related individual differences in functional connectivity falls in the spectrum of the so called "weak ties", i.e. weak connectivities within the left tail of the distribution (Santarnecchi, Galli, Polizzotto, Rossi, and Rossi 2014b), a finding which has been confirmed also in the current study (see Fig. S2). This similarity posits the suggestive idea that, like for robustness and evolvability, also intelligence might be considered a "dominant" phenotype whose biological implications are observable in terms of a better ability to cope with unexpected events.

4.2 Robustness and brain pathology

In fact, our results sustain the idea of intelligence as able to explain part of the individual differences in the robustness towards neurodegenerative or suddenly intercurring pathological conditions, suggesting a possible connection with the CR model (Stern 2009b).The idea that "some people appears to be more resilient to brain changes than others" (Stern 2012) has opened a new research field in contemporary neuroscience, aimed at understanding both the underlying mechanisms and candidate biomarkers for this buffer, with evidences also pointing at specific brain topology configurations which have been proven to be altered in pathological conditions. Interestingly, even though brain robustness has not been tested in a large number of pathological conditions, alterations in network metrics highly correlated with robustness, such as clustering coefficient, modularity and small-worldness, have been reported in schizophrenia (Bassett, Bullmore, Verchinski, Mattay, Weinberger, and Meyer-Lindenberg 2008;He et al. 2012;Yu et al. 2011), Alzheimer's disease (Reijmer, Leemans, Caeyenberghs, Heringa, Koek, and Biessels 2013;Zhao et al. 2012), autism (Belmonte, Allen, Beckel-Mitchener, Boulanger, Carper, and Webb 2004;Maximo, Keown, Nair, and Muller 2013), ADHD (Castellanos, Kelly, and Milham 2009;Castellanos and Proal 2012), and dementia (Pievani, de, Wu, Seeley, and Frisoni 2011). Furthermore, our finding suggest topological properties among those related to distributed information processing -instead of local computation- as mostly representative to the robustness-intelligence correlation, suggesting a potential framework for the ability to successfully reallocate resources behind the CR model. Interestingly, the idea ofa possible correlation between premorbid brain robustness level and individual shielding towards pathology also seems to couple together with recent contributions documenting how intelligence level effectively shapes brain networks dynamics towards a pattern strongly supporting the CR concept (Fischer, Wolf, Scheurich, and Fellgiebel 2014;Stern 2009a). While our data provide new interesting

insights in this direction, also promoting a possible age-dependent modulation of such interaction as well as partially excluding potential interaction with "brain reserve" (Bartres-Faz and Arenaza-Urquijo 2011;Stern 2002), longitudinal studies involving both healthy and pathological subjects across the life span are needed.

4.3 The intelligence-robustness interaction in the brain

The differential interaction between intelligence level and the robustness to TA and RE might reflect the network-structure idea behind these two diverse -basically opposite- types of robustness indexes. While the former process is based on targeting the most important region(s) of the brain first, thus theoretically inducing the larger disruption to the overall network integrity in just a few steps, the latter is based on a completely random targeting (Alstott, Breakspear, Hagmann, Cammoun, and Sporns 2009), leading to different network organizations which may be better shielded against one or the other procedure. Given an highly centralized system where the vast majority of the information is handled by a small subset of network nodes -like the human brain-, TA certainly represents the most dangerous configuration: stroke is a paradigmatic example, in which also its sudden occurrence might play a role in overall network dysfunction. On the other hand, the RE approach relies on the small probability that the most important regions (being just a small portion of the entire population) are being randomly targeted, making this procedure less likely to induce a dramatic network impairment, unless the lesioning process is protracted in time as in a slowly progressing neurodegenerative disease. The fact that intelligence, and more significantly FSIQ and VIQ, correlates mostly with robustness to TA inherently suggests how intelligence may interact - "shape" - brain network configuration. By implying intelligence as responsible for a more widespread and efficient brain resource allocation at rest, our results support previous observations of a positive spatial correlation

between intelligence level and brain volumes -mostly encompassing frontal, parietal and occipital lobes (Colom, Jung, and Haier 2006;Colom, Karama, Jung, and Haier 2010), contrasting the idea of prefrontal cortices as primary brain sites related to intelligence level (Duncan et al. 2000). Moreover, in the context of the CR theory, this may give reason of the better capacity to keep the network working properly on the ground a less-centralized system, where different operations may be successfully executed along different paths. However, even though this implies an increased equality across brain regions importance, a small subset of regions still could play a predominant role in more intelligent brains, leading to two interesting findings.

First of all, identified regions encompassing frontal, parietal and temporal lobes resemble those belonging to a widely recognized theory about the neuroanatomical substrate of human intelligence, that is the Parieto-Frontal Integration Theory (P-FIT) (Jung and Haier 2007) (see Figure   6). In the last few years the P-FIT has received large experimental support using a number of imaging techniques, such as structural (Narr et al. 2007), diffusion weighted (Chiang et al. 2009) and functional MRI (Choi et al. 2008;Yuan, Qin, Wang, Jiang, Zhang, and Yu 2012), circumscribing the individual variability in intelligence level to the functional coupling between prefrontal, parietal and temporal lobes regions interplay. It is therefore reasonable that the same regions also contributed to the overall intelligence-related increase in network robustness, which is in turn dependent on their centrality and global efficiency (Alstott, Breakspear, Hagmann, Cammoun, and Sporns 2009). Generally, our results confirm the idea of a primary role of parietal, frontal and temporal regions into explaining intelligence variability, meanwhile originally suggesting these very regions as also responsible for higher brain robustness in more intelligent subjects. However, whether the increase in intelligence level do trigger or, on the

contrary, results from the inherent modulation of brain networks organization -which in turn lead to an increase in robustness- remains obscure. Such hypothesis would require a longitudinal evaluation or larger cross-sectional studies in order to look at the interaction between these factors at different ages. Secondly, the subset of regions showing the higher discriminatory power between High and Low IQ subjects are integral part of the language processing network, specifically the pars-opercularis of the inferior frontal gyrus (BA44), the inferior parietal lobe (BA40) and the middle frontal gyrus (BA46) (Binder, Frost, Hammeke, Cox, Rao, and Prieto 1997b;Simos et al. 1999). Interestingly, an additional seed-based functional connectivity analysis on these language-related regions showed a peculiar difference in the functional connectivity profile of the two IQ classes, with High-IQ individuals reporting decreased within-network and increased network-rest-of-the-brain connectivity with respect to Low-IQ ones. Moreover, these regions also showed, for instance, significantly increased and decreased connectivity between working memory resting-state networks and, respectively, prefrontal and parietal regions. The interpretation of these results clearly goes beyond the intent of the present study, even though they suggest how those regions responsible for the drop in the *LCC* size may represent a core set of brain areas whose connectivity might play a role to explain IQ-related individual differences, regardless of their role for robustness. Further studies are required to explore such interaction by adopting a more in-depth battery of neuropsychological tests specifically focused on these cognitive dimensions. Moreover, fluid (G*f*, represented here as PIQ) and crystallized (G*c*, represented here as VIQ) components of intelligence did not show any significant differential interaction with brain robustness to TA. Even though verbal and performance WASI subscores can be roughly utilized as estimates of G*f* and G*c*, such distinction is not entirely part of the theoretical work behind nor the WASI (Weschler, 1999) neither its full-length counterpart WAIS

27

(Weschler, 1997). Therefore, such hypothesis should be then tested using specifically tuned instruments as well (Matzen, Benz, Dixon, Posey, Kroger, and Speed 2010;Santarnecchi et al. 2013).

4.4 Robustness as a testing platform for brain flexibility

Finally, it is noteworthy that the theoretical approach described here cannot take into account that a TA may trigger adaptive mechanisms in the living brain (i.e., brain plasticity), which usually tends to partly compensate the effects of the lesion. However, this opens new interesting scenarios where the predictive power of this kind of simulation over the actual recovery observed in patients may be tested. For instance, increasing spatial resolution of the TA may lead to the identification of fine-grained robustness-based biomarker, which may be applied in early stages of neurodegenerative processes. Moreover, the interaction between intelligence and brain resilience could also be tested in a dynamic fashion using agent-based models(Joyce, Hayaska, and Laurienti 2012;Joyce, Laurienti, and Hayasaka 2012), where the reaction of the network to the injection of a signal in a specific node is tested through time(Joyce, Hayaska, and Laurienti 2013). Within the same context, current results also open an original perspective into the understanding of the mechanisms by which brain stimulation techniques as Transcranial Magnetic Stimulation (TMS) (Barker, Jalinous, and Freeston 1985;Pascual-Leone, Walsh, and Rothwell 2000;Rossi and Rossini 2004a), transcranial Direct Current Stimulation (tDCS) or transcranial Alternate Current Stimulation (tACS) (Nitsche and Paulus 2011;Paulus 2011) might exert their actions on brain networks by physically inducing the targeted (or random) attacks we have modeled. The field of "perturbation-based imaging" is exponentially growing, both for research and clinical perspectives (Pascual-Leone et al. 2011;Rossini and Rossi 2007), based on the concept that these techniques, at experimenters' demands, can allow to both inhibit (i.e.,

"disconnect" from the system, a process which resemble our node-depletion approach) oreven enhance specific brain regions activity (Feurra, Bianco, Santarnecchi, Del, Rossi, and Rossi 2011;Rossi and Rossini 2004b;Santarnecchi et al. 2013;Terney, Chaieb, Moliadze, Antal, and Paulus 2008), with a cascade of effects over nodes belonging to the same network or even in remotely interconnected regions (Casali, Casarotto, Rosanova, Mariotti, and Massimini 2010;Massimini, Boly, Casali, Rosanova, and Tononi 2009;Polania, Paulus, Antal, and Nitsche 2011). To correlate connectivity patterns obtained using TMS-EEG or TMS-fMRI in individual with different cognitive profiles could provide insights about the relationship between brain response (in a sense, an index of "brain flexibility", which might partly account for individual responsiveness to the external perturbation) and general cognitive features, thus confirming the protective role of higher order cognitive functions.

5.0 Conclusion

Current results contribute to widen the concept of intelligence from "the substrate required to solve complex tasks" towards a factor significantly influencing several aspects of human well-being through behavioral and biological cascade effects, also promoting the evolutionary role of higher order cognition and its protective role against ageing and neurodegenerative process.

Authors Contributions

E.S. designed research; E.S. analyzed data; E.S. and S.R. critically interpreted results and wrote the paper, S.R. and A.R. supervised the study..

Reference List

ACHARD S and BULLMORE E. Efficiency and cost of economical brain functional networks. *PLoS.Comput.Biol.,* 3: e17, 2007.

ACHARD S, SALVADOR R, WHITCHER B, SUCKLING J, and BULLMORE E. A resilient, low-frequency, small-world human brain functional network with highly connected association cortical hubs. *J.Neurosci.,* 26: 63-72, 2006.

ALBERT R, JEONG H, and BARABASI AL. Error and attack tolerance of complex networks. *Nature,* 406: 378-382, 2000.

ALLEN EA, ERHARDT EB, DAMARAJU E, GRUNER W, SEGALL JM, SILVA RF, HAVLICEK M, RACHAKONDA S, FRIES J, KALYANAM R, MICHAEL AM, CAPRIHAN A, TURNER JA, EICHELE T, ADELSHEIM S, BRYAN AD, BUSTILLO J, CLARK VP, FELDSTEIN EWING SW, FILBEY F, FORD CC, HUTCHISON K, JUNG RE, KIEHL KA, KODITUWAKKU P, KOMESU YM, MAYER AR, PEARLSON GD, PHILLIPS JP, SADEK JR, STEVENS M, TEUSCHER U, THOMA RJ, and CALHOUN VD. A baseline for the multivariate comparison of resting-state networks. *Front Syst.Neurosci.,* 5: 2, 2011a.

ALLEN EA, ERHARDT EB, DAMARAJU E, GRUNER W, SEGALL JM, SILVA RF, HAVLICEK M, RACHAKONDA S, FRIES J, KALYANAM R, MICHAEL AM, CAPRIHAN A, TURNER JA, EICHELE T, ADELSHEIM S, BRYAN AD, BUSTILLO J, CLARK VP, FELDSTEIN EWING SW, FILBEY F, FORD CC, HUTCHISON K, JUNG RE, KIEHL KA, KODITUWAKKU P, KOMESU YM, MAYER AR, PEARLSON GD, PHILLIPS JP, SADEK JR, STEVENS M, TEUSCHER U, THOMA RJ, and CALHOUN VD. A baseline for the multivariate comparison of resting-state networks. *Front Syst.Neurosci.,* 5: 2, 2011b.

ALSTOTT J, BREAKSPEAR M, HAGMANN P, CAMMOUN L, and SPORNS O. Modeling the impact of lesions in the human brain. *PLoS.Comput.Biol.,* 5: e1000408, 2009.

BAK P and PACZUSKI M. Complexity, contingency, and criticality. *Proc.Natl.Acad.Sci.U.S.A,* 92: 6689-6696, 1995.

BARABASI AL and ALBERT R. Emergence of scaling in random networks. *Science,* 286: 509-512, 1999.

BARKER AT, JALINOUS R, and FREESTON IL. Non-invasive magnetic stimulation of human motor cortex. *Lancet,* 1: 1106-1107, 1985.

BARTRES-FAZ D and ARENAZA-URQUIJO EM. Structural and functional imaging correlates of cognitive and brain reserve hypotheses in healthy and pathological aging. *Brain Topogr.,* 24: 340-357, 2011.

BASSETT DS, BULLMORE E, VERCHINSKI BA, MATTAY VS, WEINBERGER DR, and MEYER-LINDENBERG A. Hierarchical organization of human cortical networks in health and schizophrenia. *J.Neurosci.,* 28: 9239-9248, 2008.

BASTIN C, YAKUSHEV I, BAHRI MA, FELLGIEBEL A, EUSTACHE F, LANDEAU B, SCHEURICH A, FEYERS D, COLLETTE F, CHETELAT G, and SALMON E. Cognitive reserve impacts on inter-individual variability in resting-state cerebral metabolism in normal aging. *Neuroimage.,* 63: 713-722, 2012.

BATTY GD, SHIPLEY MJ, GALE CR, MORTENSEN LH, and DEARY IJ. Does IQ predict total and cardiovascular disease mortality as strongly as other risk factors? Comparison of effect estimates using the Vietnam Experience Study. *Heart,* 94: 1541-1544, 2008.

BATTY GD, WENNERSTAD KM, SMITH GD, GUNNELL D, DEARY IJ, TYNELIUS P, and RASMUSSEN F. IQ in early adulthood and mortality by middle age: cohort study of 1 million Swedish men. *Epidemiology,* 20: 100-109, 2009.

BELMONTE MK, ALLEN G, BECKEL-MITCHENER A, BOULANGER LM, CARPER RA, and WEBB SJ. Autism and abnormal development of brain connectivity. *J.Neurosci.,* 24: 9228-9231, 2004.

BINDER JR, FROST JA, HAMMEKE TA, COX RW, RAO SM, and PRIETO T. Human brain language areas identified by functional magnetic resonance imaging. *J.Neurosci.,* 17: 353-362, 1997.

BULLMORE ET and BASSETT DS. Brain graphs: graphical models of the human brain connectome. *Annu.Rev.Clin.Psychol.,* 7: 113-140, 2011.

CAPPA SF. Imaging semantics and syntax. *Neuroimage.,* 61: 427-431, 2012.

CARLSON JM and DOYLE J. Highly optimized tolerance: a mechanism for power laws in designed systems. *Phys.Rev.E.Stat.Phys.Plasmas.Fluids Relat Interdiscip.Topics.,* 60: 1412-1427, 1999.

CASALI AG, CASAROTTO S, ROSANOVA M, MARIOTTI M, and MASSIMINI M. General indices to characterize the electrical response of the cerebral cortex to TMS. *Neuroimage.,* 49: 1459-1468, 2010.

CASTELLANOS FX, KELLY C, and MILHAM MP. The restless brain: attention-deficit hyperactivity disorder, resting-state functional connectivity, and intrasubject variability. *Can.J.Psychiatry,* 54: 665-672, 2009.

CASTELLANOS FX and PROAL E. Large-scale brain systems in ADHD: beyond the prefrontal-striatal model. *Trends Cogn Sci.,* 16: 17-26, 2012.

CHIANG MC, BARYSHEVA M, SHATTUCK DW, LEE AD, MADSEN SK, AVEDISSIAN C, KLUNDER AD, TOGA AW, MCMAHON KL, DE ZUBICARAY GI, WRIGHT MJ, SRIVASTAVA A, BALOV N, and THOMPSON PM. Genetics of brain fiber architecture and intellectual performance. *J.Neurosci.,* 29: 2212-2224, 2009.

CHOI YY, SHAMOSH NA, CHO SH, DEYOUNG CG, LEE MJ, LEE JM, KIM SI, CHO ZH, KIM K, GRAY JR, and LEE KH. Multiple bases of human intelligence revealed by cortical thickness and neural activation. *J.Neurosci.,* 28: 10323-10329, 2008.

COLOM R, JUNG RE, and HAIER RJ. Distributed brain sites for the g-factor of intelligence. *Neuroimage.,* 31: 1359-1365, 2006.

COLOM R, KARAMA S, JUNG RE, and HAIER RJ. Human intelligence and brain networks. *Dialogues.Clin.Neurosci.,* 12: 489-501, 2010.

CRADDOCK RC, JBABDI S, YAN CG, VOGELSTEIN JT, CASTELLANOS FX, DI MA, KELLY C, HEBERLEIN K, COLCOMBE S, and MILHAM MP. Imaging human connectomes at the macroscale. *Nat.Methods,* 10: 524-539, 2013.

DE VISSER JA, HERMISSON J, WAGNER GP, ANCEL ML, BAGHERI-CHAICHIAN H, BLANCHARD JL, CHAO L, CHEVERUD JM, ELENA SF, FONTANA W, GIBSON G, HANSEN TF, KRAKAUER D, LEWONTIN RC, OFRIA C, RICE SH, VON DG, WAGNER A, and WHITLOCK MC. Perspective: Evolution and detection of genetic robustness. *Evolution,* 57: 1959-1972, 2003.

DEARY I. Why do intelligent people live longer? *Nature,* 456: 175-176, 2008.

DEARY IJ and DER G. Reaction time explains IQ's association with death. *Psychol.Sci.,* 16: 64-69, 2005.

DEVINSKY O, MORRELL MJ, and VOGT BA. Contributions of anterior cingulate cortex to behaviour. *Brain,* 118 (Pt 1): 279-306, 1995.

DOWNES JH, HAMMOND MW, XYDAS D, SPENCER MC, BECERRA VM, WARWICK K, WHALLEY BJ, and NASUTO SJ. Emergence of a small-world functional network in cultured neurons. *PLoS.Comput.Biol.,* 8: e1002522, 2012.

DUNCAN J, SEITZ RJ, KOLODNY J, BOR D, HERZOG H, AHMED A, NEWELL FN, and EMSLIE H. A neural basis for general intelligence. *Science,* 289: 457-460, 2000.

EGUILUZ VM, CHIALVO DR, CECCHI GA, BALIKI M, and APKARIAN AV. Scale-free brain functional networks. *Phys.Rev.Lett.,* 94: 018102, 2005.

FEURRA M, BIANCO G, SANTARNECCHI E, DEL TM, ROSSI A, and ROSSI S. Frequency-dependent tuning of the human motor system induced by transcranial oscillatory potentials. *J.Neurosci.,* 31: 12165-12170, 2011.

FISCHER FU, WOLF D, SCHEURICH A, and FELLGIEBEL A. Association of structural global brain network properties with intelligence in normal aging. *PLoS.One.,* 9: e86258, 2014.

FOX MD, SNYDER AZ, VINCENT JL, CORBETTA M, VAN ESSEN DC, and RAICHLE ME. The human brain is intrinsically organized into dynamic, anticorrelated functional networks. *Proc.Natl.Acad.Sci.U.S.A,* 102: 9673-9678, 2005.

FRANK E, HALL M, TRIGG L, HOLMES G, and WITTEN IH. Data mining in bioinformatics using Weka. *Bioinformatics.,* 20: 2479-2481, 2004.

GOTTFREDSON LS. Intelligence: is it the epidemiologists' elusive "fundamental cause" of social class inequalities in health? *J.Pers.Soc.Psychol.,* 86: 174-199, 2004.

HAGMANN P, CAMMOUN L, GIGANDET X, MEULI R, HONEY CJ, WEDEEN VJ, and SPORNS O. Mapping the structural core of human cerebral cortex. *PLoS.Biol.,* 6: e159, 2008.

HAIER RJ, JUNG RE, YEO RA, HEAD K, and ALKIRE MT. Structural brain variation and general intelligence. *Neuroimage.,* 23: 425-433, 2004.

HAIER RJ, JUNG RE, YEO RA, HEAD K, and ALKIRE MT. The neuroanatomy of general intelligence: sex matters. *Neuroimage.,* 25: 320-327, 2005.

HE H, SUI J, YU Q, TURNER JA, HO BC, SPONHEIM SR, MANOACH DS, CLARK VP, and CALHOUN VD. Altered small-world brain networks in schizophrenia patients during working memory performance. *PLoS.One.,* 7: e38195, 2012.

HUMPHRIES MD and GURNEY K. Network 'small-world-ness': a quantitative method for determining canonical network equivalence. *PLoS.One.,* 3: e0002051, 2008.

JIMURA K, KONISHI S, and MIYASHITA Y. Temporal pole activity during perception of sad faces, but not happy faces, correlates with neuroticism trait. *Neurosci.Lett.,* 453: 45-48, 2009.

JOYCE KE, HAYASAKA S, and LAURIENTI PJ. The human functional brain network demonstrates structural and dynamical resilience to targeted attack. *PLoS.Comput.Biol.,* 9: e1002885, 2013.

JOYCE KE, HAYASKA S, and LAURIENTI PJ. A genetic algorithm for controlling an agent-based model of the functional human brain. *Biomed.Sci.Instrum.,* 48: 210-217, 2012.

JOYCE KE, LAURIENTI PJ, and HAYASAKA S. Complexity in a brain-inspired agent-based model. *Neural Netw.,* 33: 275-290, 2012.

JUNG RE and HAIER RJ. The Parieto-Frontal Integration Theory (P-FIT) of intelligence: converging neuroimaging evidence. *Behav.Brain Sci.,* 30: 135-154, 2007.

KIRSCHNER M and GERHART J. Evolvability. *Proc.Natl.Acad.Sci.U.S.A,* 95: 8420-8427, 1998.

KITANO H. Biological robustness. *Nat.Rev.Genet.,* 5: 826-837, 2004.

KOBAYASHI Y. [Cingulate gyrus: cortical architecture and connections]. *Brain Nerve,* 63: 473-482, 2011.

LANGDON DW. Cognition in multiple sclerosis. *Curr.Opin.Neurol.,* 24: 244-249, 2011.

LIU Y, LIANG M, ZHOU Y, HE Y, HAO Y, SONG M, YU C, LIU H, LIU Z, and JIANG T. Disrupted small-world networks in schizophrenia. *Brain,* 131: 945-961, 2008.

MANTINI D, PERRUCCI MG, DEL GC, ROMANI GL, and CORBETTA M. Electrophysiological signatures of resting state networks in the human brain. *Proc.Natl.Acad.Sci.U.S.A,* 104: 13170-13175, 2007.

MASSIMINI M, BOLY M, CASALI A, ROSANOVA M, and TONONI G. A perturbational approach for evaluating the brain's capacity for consciousness. *Prog.Brain Res.,* 177: 201-214, 2009.

MATZEN LE, BENZ ZO, DIXON KR, POSEY J, KROGER JK, and SPEED AE. Recreating Raven's: software for systematically generating large numbers of Raven-like matrix problems with normed properties. *Behav.Res.Methods,* 42: 525-541, 2010.

MAXIMO JO, KEOWN CL, NAIR A, and MULLER RA. Approaches to local connectivity in autism using resting state functional connectivity MRI. *Front Hum.Neurosci.,* 7: 605, 2013.

MORRIS JS, FRISTON KJ, BUCHEL C, FRITH CD, YOUNG AW, CALDER AJ, and DOLAN RJ. A neuromodulatory role for the human amygdala in processing emotional facial expressions. *Brain,* 121 (Pt 1): 47-57, 1998.

MURRAY AD, STAFF RT, MCNEIL CJ, SALARIRAD S, AHEARN TS, MUSTAFA N, and WHALLEY LJ. The balance between cognitive reserve and brain imaging biomarkers of cerebrovascular and Alzheimer's diseases. *Brain,* 134: 3687-3696, 2011.

NARR KL, WOODS RP, THOMPSON PM, SZESZKO P, ROBINSON D, DIMTCHEVA T, GURBANI M, TOGA AW, and BILDER RM. Relationships between IQ and regional cortical gray matter thickness in healthy adults. *Cereb.Cortex,* 17: 2163-2171, 2007.

NISBETT RE, ARONSON J, BLAIR C, DICKENS W, FLYNN J, HALPERN DF, and TURKHEIMER E. Intelligence: new findings and theoretical developments. *Am.Psychol.,* 67: 130-159, 2012.

NITSCHE MA and PAULUS W. Transcranial direct current stimulation--update 2011. *Restor.Neurol.Neurosci.,* 29: 463-492, 2011.

PAPATHANASSIOU D, ETARD O, MELLET E, ZAGO L, MAZOYER B, and TZOURIO-MAZOYER N. A common language network for comprehension and production: a contribution to the definition of language epicenters with PET. *Neuroimage.,* 11: 347-357, 2000.

PASCUAL-LEONE A, FREITAS C, OBERMAN L, HORVATH JC, HALKO M, ELDAIEF M, BASHIR S, VERNET M, SHAFI M, WESTOVER B, VAHABZADEH-HAGH AM, and ROTENBERG A. Characterizing brain cortical plasticity and network dynamics across the age-span in health and disease with TMS-EEG and TMS-fMRI. *Brain Topogr.,* 24: 302-315, 2011.

PASCUAL-LEONE A, WALSH V, and ROTHWELL J. Transcranial magnetic stimulation in cognitive neuroscience--virtual lesion, chronometry, and functional connectivity. *Curr.Opin.Neurobiol.,* 10: 232-237, 2000.

PAULUS W. Transcranial electrical stimulation (tES - tDCS; tRNS, tACS) methods. *Neuropsychol.Rehabil.,* 21: 602-617, 2011.

PAYTON A. The impact of genetic research on our understanding of normal cognitive ageing: 1995 to 2009. *Neuropsychol.Rev.,* 19: 451-477, 2009.

PENKE L, MANIEGA SM, BASTIN ME, HERNANDEZ MC, MURRAY C, ROYLE NA, STARR JM, WARDLAW JM, and DEARY IJ. Brain-wide white matter tract integrity is associated with information processing speed and general intelligence. *Mol.Psychiatry,* 17: 955, 2012a.

PIERCE A, MILLER G, ARDEN R, and GOTTFREDSON LS. Why is intelligence correlated with semen quality?: Biochemical pathways common to sperm and neuron function and their vulnerability to pleiotropic mutations. *Commun.Integr.Biol.,* 2: 385-387, 2009.

PIEVANI M, DE HW, WU T, SEELEY WW, and FRISONI GB. Functional network disruption in the degenerative dementias. *Lancet Neurol.,* 10: 829-843, 2011.

POLANIA R, PAULUS W, ANTAL A, and NITSCHE MA. Introducing graph theory to track for neuroplastic alterations in the resting human brain: a transcranial direct current stimulation study. *Neuroimage.,* 54: 2287-2296, 2011.

POLETTI M, EMRE M, and BONUCCELLI U. Mild cognitive impairment and cognitive reserve in Parkinson's disease. *Parkinsonism.Relat Disord.,* 17: 579-586, 2011.

REIJMER YD, LEEMANS A, CAEYENBERGHS K, HERINGA SM, KOEK HL, and BIESSELS GJ. Disruption of cerebral networks and cognitive impairment in Alzheimer disease. *Neurology,* 80: 1370-1377, 2013.

ROSSI S and ROSSINI PM. TMS in cognitive plasticity and the potential for rehabilitation. *Trends Cogn Sci.,* 8: 273-279, 2004a.

ROSSI S and ROSSINI PM. TMS in cognitive plasticity and the potential for rehabilitation. *Trends Cogn Sci.,* 8: 273-279, 2004b.

ROSSINI PM and ROSSI S. Transcranial magnetic stimulation: diagnostic, therapeutic, and research potential. *Neurology,* 68: 484-488, 2007.

SANTARNECCHI E, GALLI G, POLIZZOTTO NR, ROSSI A, and ROSSI S. Efficiency of weak brain connections support general cognitive functioning. *Hum.Brain Mapp.,* 2014.

SANTARNECCHI E, POLIZZOTTO NR, GODONE M, GIOVANNELLI F, FEURRA M, MATZEN L, ROSSI A, and ROSSI S. Frequency-dependent enhancement of fluid intelligence induced by transcranial oscillatory potentials. *Curr.Biol.,* 23: 1449-1453, 2013.

SATZ P, COLE MA, HARDY DJ, and RASSOVSKY Y. Brain and cognitive reserve: mediator(s) and construct validity, a critique. *J.Clin.Exp.Neuropsychol.,* 33: 121-130, 2011.

SEPULCRE J, LIU H, TALUKDAR T, MARTINCORENA I, YEO BT, and BUCKNER RL. The organization of local and distant functional connectivity in the human brain. *PLoS.Comput.Biol.,* 6: e1000808, 2010.

SHEHZAD Z, KELLY C, REISS PT, CAMERON CR, EMERSON JW, MCMAHON K, COPLAND DA, CASTELLANOS FX, and MILHAM MP. A multivariate distance-based analytic framework for connectome-wide association studies. *Neuroimage.,* 93 Pt 1: 74-94, 2014.

SIMOS PG, PAPANICOLAOU AC, BREIER JI, WHELESS JW, CONSTANTINOU JE, GORMLEY WB, and MAGGIO WW. Localization of language-specific cortex by using magnetic source imaging and electrical stimulation mapping. *J.Neurosurg.,* 91: 787-796, 1999.

SPORNS O. Network attributes for segregation and integration in the human brain. *Curr.Opin.Neurobiol.,* 2013.

SPORNS O. Contributions and challenges for network models in cognitive neuroscience. *Nat.Neurosci.,* 2014.

SPORNS O, TONONI G, and EDELMAN GM. Theoretical neuroanatomy and the connectivity of the cerebral cortex. *Behav.Brain Res.,* 135: 69-74, 2002.

SPORNS O and ZWI JD. The small world of the cerebral cortex. *Neuroinformatics.,* 2: 145-162, 2004.

STERN Y. What is cognitive reserve? Theory and research application of the reserve concept. *J.Int.Neuropsychol.Soc.,* 8: 448-460, 2002.

STERN Y. Cognitive reserve. *Neuropsychologia,* 47: 2015-2028, 2009.

STERN Y. Cognitive reserve in ageing and Alzheimer's disease. *Lancet Neurol.,* 11: 1006-1012, 2012.

TERNEY D, CHAIEB L, MOLIADZE V, ANTAL A, and PAULUS W. Increasing human brain excitability by transcranial high-frequency random noise stimulation. *J.Neurosci.,* 28: 14147-14155, 2008.

TZOURIO-MAZOYER N, LANDEAU B, PAPATHANASSIOU D, CRIVELLO F, ETARD O, DELCROIX N, MAZOYER B, and JOLIOT M. Automated anatomical labeling of activations in SPM using a macroscopic anatomical parcellation of the MNI MRI single-subject brain. *Neuroimage.,* 15: 273-289, 2002.

VAN DEN HEUVEL MP, KAHN RS, GONI J, and SPORNS O. High-cost, high-capacity backbone for global brain communication. *Proc.Natl.Acad.Sci.U.S.A,* 109: 11372-11377, 2012.

VAN DEN HEUVEL MP and SPORNS O. An anatomical substrate for integration among functional networks in human cortex. *J.Neurosci.,* 33: 14489-14500, 2013.

VAN DEN HEUVEL MP, STAM CJ, KAHN RS, and HULSHOFF POL HE. Efficiency of functional brain networks and intellectual performance. *J.Neurosci.,* 29: 7619-7624, 2009.

WANG L, LI Y, METZAK P, HE Y, and WOODWARD TS. Age-related changes in topological patterns of large-scale brain functional networks during memory encoding and recognition. *Neuroimage.,* 50: 862-872, 2010.

WATTS DJ and STROGATZ SH. Collective dynamics of 'small-world' networks. *Nature,* 393: 440-442, 1998.

WU K, TAKI Y, SATO K, HASHIZUME H, SASSA Y, TAKEUCHI H, THYREAU B, HE Y, EVANS AC, LI X, KAWASHIMA R, and FUKUDA H. Topological organization of functional brain networks in healthy children: differences in relation to age, sex, and intelligence. *PLoS.One.,* 8: e55347, 2013.

YU Q, SUI J, RACHAKONDA S, HE H, GRUNER W, PEARLSON G, KIEHL KA, and CALHOUN VD. Altered topological properties of functional network connectivity in schizophrenia during resting state: a small-world brain network study. *PLoS.One.,* 6: e25423, 2011.

YUAN Z, QIN W, WANG D, JIANG T, ZHANG Y, and YU C. The salience network contributes to an individual's fluid reasoning capacity. *Behav.Brain Res.,* 229: 384-390, 2012.

ZHAO X, LIU Y, WANG X, LIU B, XI Q, GUO Q, JIANG H, JIANG T, and WANG P. Disrupted small-world brain networks in moderate Alzheimer's disease: a resting-state FMRI study. *PLoS.One.,* 7: e33540, 2012.

ZIHL J, FINK T, PARGENT F, ZIEGLER M, and BUHNER M. Cognitive reserve in young and old healthy subjects: differences and similarities in a testing-the-limits paradigm with DSST. *PLoS.One.,* 9: e84590, 2014.

FIGURES AND TABLES LEGENDS

Fig.1.Functional MRI preprocessing and graph-topological brain resilience analysis workflow. Schematic representation of the major steps for brain resilience estimation, involving images preprocessing, thresholding procedure based on connectivity strength and topology indices computation. Panel A:functional images underwent canonical preprocessing involving two different approaches for motion correction, removal of possible confounding factors related to breathing and cardiac signals, temporal band-pass filtering, coregistration and spatial normalization using the DARTEL module for SPM. The Anatomical Labeling Atlas (AAL) was used for resting-state parcellation into regions of interest and consequent BOLD signal time series extraction. In order to retain only significant connections (Panel B, upper line), a one-sample t-test was applied over individual connectivity matrices obtained during the thresholding process (n=100), which has been computed for the entire sparsity range (1-100%) using 1% sparsity steps. Matrices followed two separated workflows for Targeted Attacks (TA) and Random Error (RE) simulations. In order to normalize graph topology indices (Panel B, lower line), a Hirschberger-Qi-Steuer algorithm was used to create transitivity-preserved null networks based on random correlation matrices matched for degree-distribution. All steps were performed at the single subject level. Additional details about topology indices estimation and lesioning procedure are provided in supplemental methods.

Fig.2. Brain Robustness and Intelligence correlation. Panel A: correlations between Full-scale (FSIQ), Verbal (VIQ) and Performance (PIQ) Intelligence Quotients(obtained at the WASI test, *x* axis) and brain robustness to TA and RE, expressed as the average size of the largest connected component (LCC, *y* axis) in the network after a the lesioning procedure. Histograms (in grey) represent data distribution in the overall sample for FSIQ, as well as *LCC* values, for both TA and RE simulations. Panel B: the lesioning procedure has been computed within the entire sparsity windows, by retaining an increasing percentage of all possible connections in a decreasing-strength fashion, thus ranging from 1% (absolute stronger connections) to 100% (*x* axis). However, as commonly applied for graph-theoretical analysis, correlations with IQ scores have been performed by using connectivity data within each subject's small-world sparsity window (group average = 10%-31%). Therefore, scatterplots in A and line plots in B refer to the *LCC* size calculated within such window, while surface plots in B, as well as data in C and D, display results for the entire sparsity range. As visible in the surface plots, *LCC* values for TA and RE follow different distributions along the sparsity windows, showing most of the individual differences within the low-sparsity range for RE and 70-90% window for TA. As shown in C (data are grouped into sparsity deciles), this produces different correlation patterns for the two robustness indexes, with an opposite pattern of correlation (Pearson's product-moment correlation coefficient) for the last two sparsitydeciles during TA simulation, an effect which is mostly driven by the inclusion of brain weak connections. At a higher resolution level, panel D shows positive (red) and negative (blue) correlations between intelligence quotients and *LCC* as a function of sparsity and % of nodes removed from the network.

Fig.3. Brain Regions responsible for robustness differences. Panel A shows brain regions responsible for higher robustness in High- vs Low-IQ participants during TA simulation, as identified by usingsupport vector machine classification. These regions, mainly represented in the bilateral frontal, parietal and temporal lobes, contributed the most in the drop of robustness (decrease in the size of the *LCC*) after their removal from the network, with an average drop in *LCC* size equal to 14 nodes. Conversely, a smaller set of regions was also identified as responsible for a greater drop in robustness in Low-IQ participants vs High-IQ ones (B). Moreover, a plot of the average drop (see colorbar) for each brain region of the AAL atlas (*x* axis) across the small-worldness sparsity range (*y* axis) is provided in panel C separately for the two groups. Accordingly to panel A, regions belonging to frontal, temporal and parietal lobes (mostly resembling the P-Fit model of intelligence) vehicle the most important robustness-related connections in subjects with higher intelligence quotients.
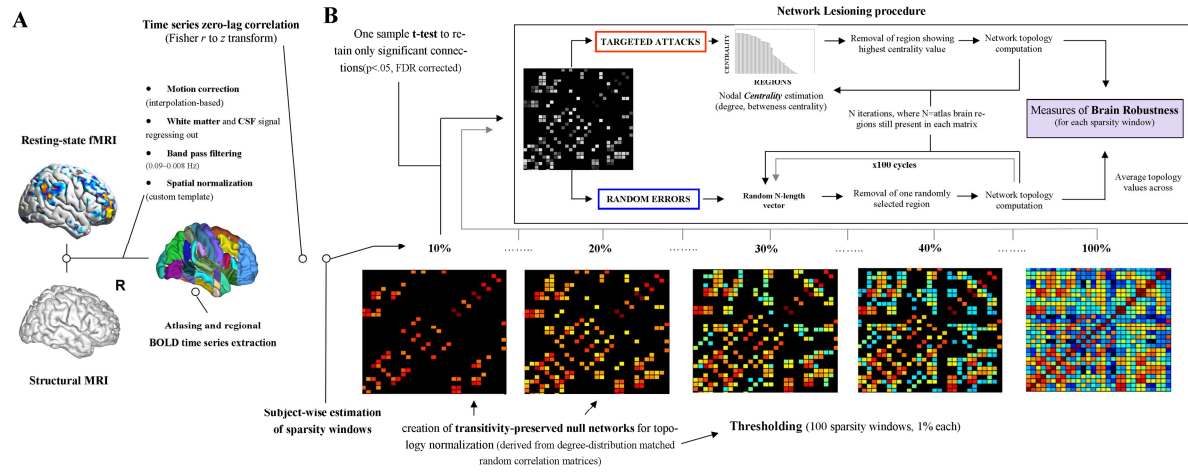
Fig.4. Pairwise functional connectivity and seed-to-network analysis results. Panel A shows no differences in the average size of the LCC in male and female participants, ruling out the hypothesis of a gender-effect as responsible for the major involvement of language-related regions (BA40, 44 and 46) into High and Low-IQ individuals discrimination, while a difference in the pairwise connectivity profile referring to frontal, limbic and parietal lobes emerged (B)(colorcode represent differences in functional connectivity - FC). A subsequent seed-based connectivity analysis based on those regions responsible for the largest drop in *LCC* size in High and Low-IQ participants has been performed, with the results for language-related regions reported in panel C. Interestingly, a pattern of decreased between-regions connectivity,as well an increased long-range, mostly inter-hemispheric connections for participants with higher IQ were identified (C, $p.<0.05$; results for remaining regions are included in Figure S5). Moreover an additional connectivity analysis between the regions responsible for the largest LCC drop in High-IQ participants and anatomically-defined resting-state networks (RSN) has been tested: this, showed a region-specific pattern of group differences in connectivity, mostly involving left and right working memory (WM), frontal attention (FA) and fronto-parietal control (FPC) networks. *indicate statistically significant IQ-related differences in seed-to-RSN correlation coefficient ($p.<0.05$, Bonferronicorrected).

Fig.5 Functional connectivity analysis in regions responsible for greater *LCC* drop in Low-IQ participants. Panel A and B respectively show the results of seed-to-RSN and pairwise functional connectivity analyses for regions shown in Figure 1B (i.e. left amygdala, left temporal pole and right anterior cingulate cortex - ACC).Increased connectivity in Low-IQ participants between amygdala and both DMN and right WM network were identified, as well as increased connectivity between left ACC and the Fronto Parietal Control Network (FPCN). [*]indicates statistically significant IQ-related differences in seed-to-RSN correlation coefficient (p.<0.05, Bonferroni corrected).

Fig. 6. The P-FIT network of human intelligence. The most relevant brain regions (Broadmann areas) belonging to the Parieto-Frontal Integration Theory network are plotted on an inflated brain surface. The figure shows both the overall bilateral network and a subsample composed solely by those regions being present uniquely on the left hemisphere (left-lateralized component) and highly resembling the network identify in High-IQ individuals. Numbers represent Brodmann areas.

50

	Overall dataset		High IQ		Low IQ		ANOVA main effect	
	M_{102}	SD_{102}	M_{102}	SD_{102}	M_{102}	SD_{102}	F	*sig.*
FSIQ	114	11	119	7	84	5	156.234	<0.001
VIQ	111	9	116	5	89	9	16.235	<0.01
PIQ	109	11	121	6	86	6	94.213	<0.001
BD	54	9	65	4	40	5	129.143	<0.001
VOC	56	9	61	6	52	9	9.552	<0.01
SIM	52	7	58	5	43	9	25.67	<0.01
MAT	51	6	62	5	46	6	59.511	<0.001

Table 1. Average values for Full scale (FSIQ), Performance (PIQ) and Verbal IQs (VIQ) both for the overall sample and for High and Low-IQ groups. Main effects of between group ANCOVA are reported (covariates of age and total brain volume), post-hoc comparisons were all significant (p<.05, Bonferroni corrected). Legend: BD=block design; VOC=vocabulary; SIM=similarities; MAT=visuo-spatial abstract reasoning matrices.

A

Time series zero-lag correlation
(Fisher *r* to *z* transform)

• **Motion correction**
(interpolation-based)

• **White matter** and CSF signal
regressing out

• **Band pass filtering**
(0.09–0.008 Hz)

• **Spatial normalization**
(custom template)

Resting-state fMRI

R

Atlasing and regional
BOLD time series extraction

Structural MRI

B

One sample **t-test** to re-
tain only significant connec-
tions(p<.05, FDR corrected)

Network Lesioning procedure

TARGETED ATTACKS

CENTRALITY

REGIONS

Nodal *Centrality* estimation
(degree, betweenness centrality)

Removal of region showing
highest centrality value

Network topology
computation

N iterations, where N=atlas brain re-
gions still present in each matrix

Measures of Brain Robustness
(for each sparsity window)

RANDOM ERRORS

x100 cycles

Random N-length
vector

Removal of one randomly
selected region

Network topology
computation

Average topology
values across

10% .... 20% .... 30% .... 40% 100%

**Subject-wise estimation
of sparsity windows**

creation of **transitivity-preserved null networks** for topo-
logy normalization (derived from degree-distribution matched
random correlation matrices)

Thresholding (100 sparsity windows, 1% each)

A

R

Largest LCC drop in High-IQ

B

R

Largest LCC drop in Low-IQ

■ Sup. Frontal Gyrus - medial (BA8)   ■ Inf. Parietal Lobe (BA40)   ■ Mid. Frontal Gyrus (BA46)

■ Inf. Temporal Lobe (BA20)   ■ Sup. Frontal Gyrus (BA6)   ■ Mid. Temporal Lobe (BA21)

■ Mid. Frontal Gyrus - pars orb. (BA11)   ■ Post. Cingulate Cortex (BA23)   ■ Inf. Frontal Gyrus - pars operc. (BA44)

■ Anterior Cingulate Cortex (BA32)   ■ Temporal Pole (BA38)   ■ Amigdala

C

High IQ   Low IQ   LCC drop

31%   31%

Network density   Network density

10%   10%

Parieto-Frontal Integration Theory Network of Intelligence
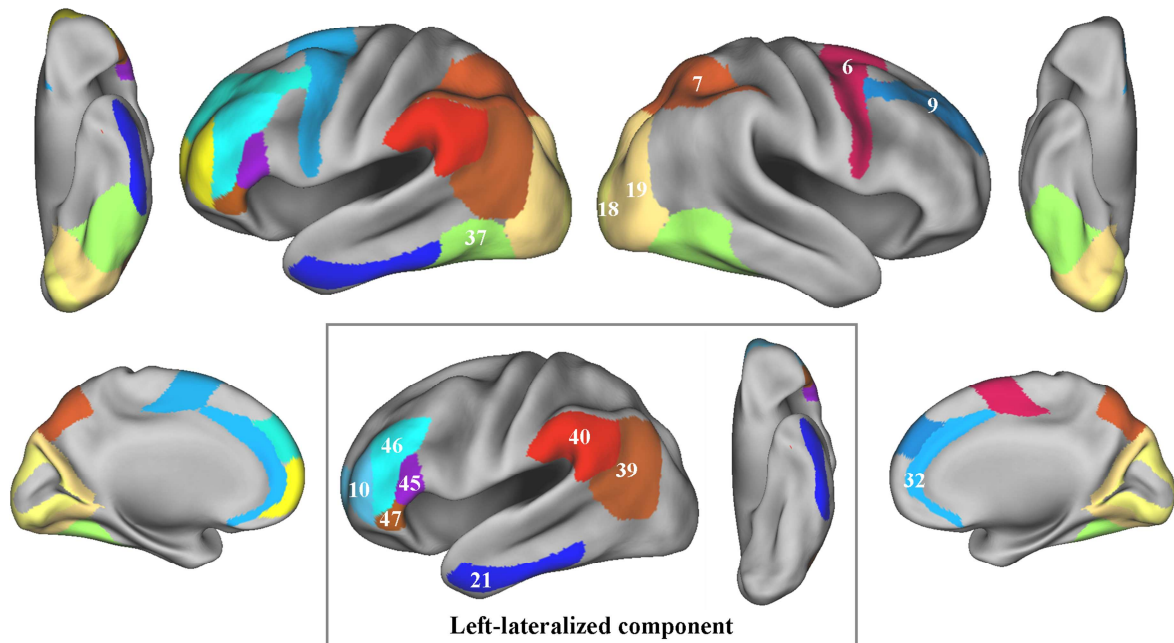
Left-lateralized component

The Smarter, the Stronger: Intelligence Level Correlates With Brain Resilience To Systematic Insults

Emiliano Santarnecchi[1-2]*, Simone Rossi[1], Alessandro Rossi[1].

[1] Department of Medicine, Surgery and Neuroscience, Neurology and Clinical Neurophysiology Section, Brain Investigation & Neuromodulation Lab., University of Siena, Italy

[2] Berenson-Allen Center for Non-Invasive Brain Stimulation, Beth Israel Medical Center, Harvard Medical School, Boston, MA, USA

Abbreviated title: Intelligence and brain robustness

Supplemental Material and Methods

- *Sample and behavioral measures*

- *Intelligence scores*

- *fMRI data acquisition*

- *fMRI data preprocessing*

- *Network analysis*

Supplemental Results

- *Correlation between Intelligence and different robustness indexes*
- *Age related differences*

Supplemental materials and methods

1.1 Intelligence scores

Intellectual performance measure included in the INDI refers to the Wechsler Abbreviated Scale of Intelligence (WASI) (Weschler, 1999). WASI is a shortened version of both the Wechsler Adult Scale of Intelligence (WAIS-III) (Weschler, 1997), and the Wechsler Intelligence Scale for Children (WISC-IV) (Weschler, 2003). Despite the use of one or multiple scores arising from a scale may oversimplify the complex concept of intelligence, this quantification was needed to obtain a standardized, statistically reliable estimation of individual overall cognitive profile to be correlated with brain robustness. The WASI consists of four subscales - Vocabulary, Similarities, Block Design and Matrix Reasoning - leading to three different scores: a standardized, full-scale intelligence quotient (FSIQ); a verbal IQ score (VIQ) which indexes word knowledge, verbal reasoning and concept formation; as well a performance IQ score (PIQ) representing abstract reasoning skills, visual information processing, visual-motor coordination, simultaneous processing and learning abilities (see Figure S1 for the results of a principal component analysis computed on the behavioural data used in the robustness analysis). The psychometric properties of the WASI include high concurrent validity, demonstrated by strong correlations with the WAIS-III FSIQ (r=.92; n=248), as well as good reliability coefficients ranging from .92 to .98 for VIQ, .94 to .97 for PIQ, .96 to .98 for the full FSIQ (Ryan, Carruthers, Miller, Souheaver, Gontkovsky, and Zehr 2003).

1.2 fMRI data acquisition

Imaging data were acquired on a 3.0 T Siemens MAGNETOM TrioTim (Siemens, Netherlands). A three-dimensional T1-weighted MPRAGE image was acquired in the axial plane (TR/TE 2500/3.5ms; 192 slices; slice thickness 1mm; flip angle 8°; voxel size 1.0×1.0×1.0 m). Resting-state fMRI data was acquired using T2-weighted BOLD images (TR/TE 2500/30ms; 38 interleaved slices; 260 volumes; slice thickness 3mm; flip angle 80°; voxel size 3.0×3.0×3.0 mm). Fieldmaps were also available for each participant fMRI scan.

1.3 fMRI data preprocessing

Neuroimaging data were preprocessed and analyzed at the department of Medicine, Surgery and Neuroscience of the University of Siena. Functional images preprocessing was carried out using a custom-made pipeline based on MATLAB scientific computing environment (http://www.mathworks.com, MathWorks, MA, USA), integrating several script for preprocessing freely available for SPM8 (Wellcome Department of Cognitive Neurology, Institute of Neurology, University College London; http://www.fil.ion.ucl.ac.uk/spm/). The first five volumes of functional images were discarded for each subject to allow for steady-state magnetization. Echo-Planar Images were (i) corrected for inhomogeneity using fieldmaps regression, then (ii) stripped of skull and other non-cerebral tissues, (iii) slice-timed using interleaved descending acquisition, (iv) realigned and (v) resliced to the mean volume for head motion correction. Two recent studies suggested that head motion during MRI scanning may produces significant changes on functional connectivity estimation and consequently over local and global topological indexes used for brain robustness quantification (Power, Barnes, Snyder,

3

Schlaggar, and Petersen 2012;Van Dijk, Sabuncu, and Buckner 2012). To tackle this issue we proceeded using the time series interpolation procedure based on displacement indexes proposed by Power and colleagues (2012), i.e. Frame-wise displacement (FD) and RMS variance of the temporal derivative (DVARS). Therefore, functional time points showing FD > 0.5 mm and DVARS > 0.5 have been interpolated using a cubic spline function. Structural images were co-registered to the mean volume of functional images and subsequently segmented using routine in SPM8. Hidden Markov Random Field model was applied in order to remove isolated voxels. To obtain a more accurate spatial normalization we applied the SPM8 DARTEL (Diffeomorphic Anatomical Registration Through Exponentiated Lie) (Ashburner 2007) module, creating a customized gray matter template from all subjects' segmented images. A nonlinear normalization procedure with subsequent affine-only normalization to the Montreal Neurological Institute (MNI) template brain, and voxel resampling to an isotropic 3x3x3 mm voxel size were then applied to functional images. Linear trends were removed to reduce the influence of the rising temperature of the MRI scanner and all functional volumes were band-pass filtered at .01 Hz<f<.08 Hz to reduce low-frequency drifts.

Finally, an important issue for brain connectivity and topology estimation is related to the deconvolution of potential confounding signals - mainly physiological high frequency respiratory and cardiac noise - from the grey matter time courses (Biswal et al. 2010). Here we opted to regress out motion parameters and signal derived from four regions-of-interest (ROIs) placed in the white matter and cerebro-spinal fluid (CSF), with this approach being proved effective in enhancing within-subject and test-retest reliability (at 45 minutes and 5-16 months) (Liang et al. 2012;Schwarz and McGonigle 2011).

1.4 Overview of network analysis

Network nodes were defined by parcellating the brain into 90 cortical and subcortical Regions of Interest (ROIs) according to the Automatic Anatomical Labeling atlas (AAL) (Tzourio-Mazoyer et al. 2002), one of the most commonly employed atlas for network analyses (Achard and Bullmore 2007;Achard, Salvador, Whitcher, Suckling, and Bullmore 2006;Liu et al. 2008;Wang, Li, Metzak, He, and Woodward 2010). The computation of topological properties requires the creation of a so-called adjacency matrix, which graphically represents the overall brain organization in terms of nodes (brain regions) and edges (representing the statistical dependency between the BOLD time series of each pair of brain regions). Therefore, adjacency matrices have been obtained for each subject by computing the pairwise zero-lag correlation coefficients ("r") between the mean BOLD time series of all possible voxels inside AAL atlas regions, leading to a 90x90 matrix with 4005 edges, i.e. connections. Given the bivariate normal distribution of correlation coefficients, r values have been "normalized" through the Fisher r to z transformation, with these normalized edges representing the whole range of possible functional links between cortical and/or subcortical regions, covering both strong (r>0.7), weak (r<0.2>0) and negative ones (r=<0). Graph topology literature suggests how the human brain shows specific properties which make feasible to obtain, at the same time, high level of both local and distributed information processing (Sporns 2013). Furthermore, several studies have shown how these properties, for instance modularity and small-worldness, may be better identified and reliably quantified by analyzing thresholded version of the full adjacency matrix, which basically corresponds to a partial representation of overall brain connections above a predetermined r value (Achard, Salvador, Whitcher, Suckling, and Bullmore 2006;Bullmore and Bassett 2011;Sporns and Zwi 2004). This thresholding process implies the creation of several,

5

progressive matrices, each comprising an increasing number of connections (Bullmore and Bassett 2011;He et al. 2009;Sporns and Zwi 2004). Practically, a full matrix will be composed by all the correlation values between each pair of regions, whereas a matrix with a threshold equal to 5% (sparsity = 5%), will be composed by a few connections representing the 5% of the most strong connections in the brain. The application of such procedure in a group of individuals leads to the creation of a series of equi-sparse networks, that is, networks of the same size retaining the same fraction of the maximum possible number of connections for each subject (5%) (Achard, Salvador, Whitcher, Suckling, and Bullmore 2006;Bassett, Bullmore, Verchinski, Mattay, Weinberger, and Meyer-Lindenberg 2008;Hayasaka and Laurienti 2010). Compared to other thresholding approaches (e.g., equi-threshold solution), this approach is thought to reduce between-subject variability in network parameters (Hayasaka and Laurienti 2010), and has therefore been widely used for complex networks characterization (Bullmore and Bassett 2011).

The distribution of correlation coefficients physiologically varies between subjects, and its shape is implicitly responsible of network properties organization (Schwarz and McGonigle 2011;Zalesky, Fornito, and Bullmore 2012). Given that it may affect brain robustness computation, consequently, we based our analysis on individual thresholded matrices instead of group average connection strengths values. Moreover, an important issue in network topology estimation arises with the high dimensionality of resting-state fMRI dataset, that is the determination of the actual proportion of real *vs* non-significant connections present in connectivity/adjacency matrix (Zalesky, Cocchi, Fornito, Murray, and Bullmore 2012). To ensure that topological features are computed upon statistically reliable connections, a one-sample t-test has been computed on each matrix for each participant. Only connections surviving

the False Discovery Rate (FDR, $p<.05$) correction for multiple comparisons entered the network lesioning process.

1.5 Determine the sparsity range for group comparisons

Several studies suggest to restrict the brain topology analysis to a specific subset of sparsity values, which represent those where brain network display the SW behavior (Achard, Salvador, Whitcher, Suckling, and Bullmore 2006;Sporns and Zwi 2004). Even though we computed and report robustness estimates along the entire sparsity window (1-100%) (see Fig. 2 C-D), ANCOVA has been conducted on data referring to individual SW window, which at the group level corresponded to sparsity values ranging from 10% to 31% of all possible connections (see Fig. 2B).

1.6 Network topology normalization

The analysis of complex networks topological organization requires the comparisons of properties of interest with those of randomly rewired networks having the same degree distribution (Maslov and Sneppen 2002). A recent study by Zalensky and colleagues (Zalesky, Fornito, and Bullmore 2012) has suggested how correlation-based networks, like the one usually utilized for brain-networks study, show an inherent structure which leads to an overestimation of network small-worldness, with these networks being inherently more clustered than random networks. This is mostly due to the implicit overestimation of direct connection between pairs of nodes where a strong indirect connection involving a third node is present, a phenomena known as *transitivity*. Correlation-based networks thus show a higher tendency to fall into the small-

world regime, with implicit consequences also for the estimation of other network properties such as modularity, centrality or motif counts. Practically, random rewiring processes imply a loss of information about both the intrinsic data structures and the "transitivity" information hold by correlation-based networks, which should be instead preserved in order to allow a reliable comparison. We therefore adopted an approach proposed by Zalensky and colleagues consisting of creating a set of null networks directly related to participants original correlation matrices. We therefore used the Hirschberger-Qi-Steuer (H-Q-S) algorithm (Hirschberger et al., 2004) to randomly generate null correlation matrices matched with the distribution of each matrix. Their respective topological properties have been calculated and applied for empirical data normalization, recursively for each participant.

1.7 Resting-State Networks definition

Resting-state networks were defined using anatomical masks as published by (Shirer, Ryali, Rykhlevskaia, Menon, and Greicius 2012). The original ROIs have been created by applying FSL's MELODIC independent component analysis (ICA) software to the group-level resting-state data of a cohort of healthy subjects. Of the 30 components generated, 14 were selected visually as being Indipendent Components based on previous reports by several authors (Fox, Snyder, Vincent, Corbetta, Van Essen, and Raichle 2005;Greicius, Krasnow, Reiss, and Menon 2003) (Smith et al. 2009). In order to avoid to capture activity from white matter, CSF or other not-grey matter tissues, we masked each RSN using individual grey matter masks of each subjects included in our study. Moreover, in order to avoid the presence of not-overlapping regions between the two anatomical parcellation schemes (RSNs and AAL) which could

8

generate unspecific source of correlation, we also masked each RSN map using the AAL atlas used for robustness analysis.

Supplemental Results

2.1 Correlation between Intelligence and different robustness indexes

Compared to *LCC*, other topological properties (*E*, E_{Loc}, *Bc)* showed less significant - as well not significant- results for both TA and RE. Since brain robustness towards TA has been computed using *Bc* values as the main criteria for target selection, regression models have been computed for all the other metrics except for *Bc* in order to avoid potential recursiveness: [TA] (i) *E* = FSIQ [$r_{(101)}$ =.45, p<.05, R^2=.16], VIQ [$r_{(101)}$ =.40, p<.05, R^2=.16] and PIQ [$r_{(101)}$ = .34, p<.05, R^2=.09], (ii) E_{Loc} = [$r_{(101)}$ =.37, p<.05, R^2=.09], VIQ [$r_{(101)}$ =.34, p<.05, R^2=.09] and PIQ [$r_{(101)}$ = .29, p<.05, R^2=.08]; [RE] (i) *E* = FSIQ [$r_{(101)}$ =.28, n.s.], VIQ [$r_{(101)}$ =.19, p<.05, R^2=.03] and PIQ [$r_{(101)}$ = .13, n.s.], (ii) E_{Loc} = [$r_{(101)}$ =.21, n.s.], VIQ [$r_{(101)}$ =.19, n.s.] and PIQ [$r_{(101)}$ = .17, n.s.]; (iii) *Bc* = [$r_{(101)}$ =.34, p<.05, R^2=.09], VIQ [$r_{(101)}$ =.33, p<.05, R^2=.09] and PIQ [$r_{(101)}$ = .25, p<.05, R^2=.08]. These results confirmed LCC as the most sensitive metric for the understanding of network response to TA and RE (Albert, Jeong, and Barabasi 2000;Alstott, Breakspear, Hagmann, Cammoun, and Sporns 2009), therefore LCC has been exclusively used in subsequent analyses.

2.2 Age related differences

While the analysis of LCC values across decades (Fig. S3) confirmed between groups (IQ, [TA] $F_{(1)}$ = 3.21, p = .013; [RE] $F_{(1)}$ = 2.13, p = .039) and age related (Decades, [TA] $F_{(4)}$ = 2.78, p = .029; [RE] $F_{(4)}$ = 1,98 p = .042) differences in both TA and RE data, the interaction

between age, intelligence and brain robustness didn't reach statistical significance for RE data $(F_{(3)} = 0.77 \, p = .276)$. However, there was a trend for significance for TA ones $(F_{(3)} = 1.21, p = .093)$. This suggests the need for further investigation on larger, perfectly balanced samples, possibly including extensive intelligence data for older subjects (>70yrs)."

Reference List

ACHARD S and BULLMORE E. Efficiency and cost of economical brain functional networks. *PLoS.Comput.Biol.,* 3: e17, 2007.

ACHARD S, SALVADOR R, WHITCHER B, SUCKLING J, and BULLMORE E. A resilient, low-frequency, small-world human brain functional network with highly connected association cortical hubs. *J.Neurosci.,* 26: 63-72, 2006.

ALBERT R, JEONG H, and BARABASI AL. Error and attack tolerance of complex networks. *Nature,* 406: 378-382, 2000.

ALSTOTT J, BREAKSPEAR M, HAGMANN P, CAMMOUN L, and SPORNS O. Modeling the impact of lesions in the human brain. *PLoS.Comput.Biol.,* 5: e1000408, 2009.

ANTAL A, BOROS K, POREISZ C, CHAIEB L, TERNEY D, and PAULUS W. Comparatively weak after-effects of transcranial alternating current stimulation (tACS) on cortical excitability in humans. *Brain Stimul.,* 1: 97-105, 2008.

ANTAL A and PAULUS W. Investigating neuroplastic changes in the human brain induced by transcranial direct (tDCS) and alternating current (tACS) stimulation methods. *Clin.EEG.Neurosci.,* 43: 175, 2012.

ANTAL A, PAULUS W, and NITSCHE MA. Electrical stimulation and visual network plasticity. *Restor.Neurol.Neurosci.,* 29: 365-374, 2011.

ASHBURNER J. A fast diffeomorphic image registration algorithm. *Neuroimage.,* 38: 95-113, 2007.

BASSETT DS, BULLMORE E, VERCHINSKI BA, MATTAY VS, WEINBERGER DR, and MEYER-LINDENBERG A. Hierarchical organization of human cortical networks in health and schizophrenia. *J.Neurosci.,* 28: 9239-9248, 2008.

BISWAL BB, MENNES M, ZUO XN, GOHEL S, KELLY C, SMITH SM, BECKMANN CF, ADELSTEIN JS, BUCKNER RL, COLCOMBE S, DOGONOWSKI AM, ERNST M, FAIR D, HAMPSON M, HOPTMAN MJ, HYDE JS, KIVINIEMI VJ, KOTTER R, LI SJ, LIN CP, LOWE MJ, MACKAY C, MADDEN DJ, MADSEN KH, MARGULIES DS, MAYBERG HS, MCMAHON K, MONK CS, MOSTOFSKY SH, NAGEL BJ, PEKAR JJ, PELTIER SJ, PETERSEN SE, RIEDL V, ROMBOUTS SA, RYPMA B, SCHLAGGAR BL, SCHMIDT S, SEIDLER RD, SIEGLE GJ, SORG C, TENG GJ, VEIJOLA J, VILLRINGER A, WALTER M, WANG L, WENG XC, WHITFIELD-GABRIELI S, WILLIAMSON P, WINDISCHBERGER C, ZANG YF, ZHANG HY, CASTELLANOS FX, and MILHAM MP. Toward discovery science of human brain function. *Proc.Natl.Acad.Sci.U.S.A,* 107: 4734-4739, 2010.

BULLMORE ET and BASSETT DS. Brain graphs: graphical models of the human brain connectome. *Annu.Rev.Clin.Psychol.,* 7: 113-140, 2011.

FOX MD, SNYDER AZ, VINCENT JL, CORBETTA M, VAN ESSEN DC, and RAICHLE ME. The human brain is intrinsically organized into dynamic, anticorrelated functional networks. *Proc.Natl.Acad.Sci.U.S.A,* 102: 9673-9678, 2005.

GREICIUS MD, KRASNOW B, REISS AL, and MENON V. Functional connectivity in the resting brain: a network analysis of the default mode hypothesis. *Proc.Natl.Acad.Sci.U.S.A,* 100: 253-258, 2003.

HAYASAKA S and LAURIENTI PJ. Comparison of characteristics between region-and voxel-based network analyses in resting-state fMRI data. *Neuroimage.,* 50: 499-508, 2010.

HE Y, WANG J, WANG L, CHEN ZJ, YAN C, YANG H, TANG H, ZHU C, GONG Q, ZANG Y, and EVANS AC. Uncovering intrinsic modular organization of spontaneous brain activity in humans. *PLoS.One.,* 4: e5226, 2009.

LIANG X, WANG J, YAN C, SHU N, XU K, GONG G, and HE Y. Effects of different correlation metrics and preprocessing factors on small-world brain functional networks: a resting-state functional MRI study. *PLoS.One.,* 7: e32766, 2012.

LIU Y, LIANG M, ZHOU Y, HE Y, HAO Y, SONG M, YU C, LIU H, LIU Z, and JIANG T. Disrupted small-world networks in schizophrenia. *Brain,* 131: 945-961, 2008.

MASLOV S and SNEPPEN K. Specificity and stability in topology of protein networks. *Science,* 296: 910-913, 2002.

POWER JD, BARNES KA, SNYDER AZ, SCHLAGGAR BL, and PETERSEN SE. Spurious but systematic correlations in functional connectivity MRI networks arise from subject motion. *Neuroimage.,* 59: 2142-2154, 2012.

RYAN JJ, CARRUTHERS CA, MILLER LJ, SOUHEAVER GT, GONTKOVSKY ST, and ZEHR MD. Exploratory factor analysis of the Wechsler Abbreviated Scale of Intelligence (WASI) in adult standardization and clinical samples. *Appl.Neuropsychol.,* 10: 252-256, 2003.

SCHWARZ AJ and MCGONIGLE J. Negative edges and soft thresholding in complex network analysis of resting state functional connectivity data. *Neuroimage.,* 55: 1132-1146, 2011.

SHIRER WR, RYALI S, RYKHLEVSKAIA E, MENON V, and GREICIUS MD. Decoding subject-driven cognitive states with whole-brain connectivity patterns. *Cereb.Cortex,* 22: 158-165, 2012.

SMITH SM, FOX PT, MILLER KL, GLAHN DC, FOX PM, MACKAY CE, FILIPPINI N, WATKINS KE, TORO R, LAIRD AR, and BECKMANN CF. Correspondence of the brain's functional architecture during activation and rest. *Proc.Natl.Acad.Sci.U.S.A,* 106: 13040-13045, 2009.

SPORNS O. Network attributes for segregation and integration in the human brain. *Curr.Opin.Neurobiol.,* 2013.

SPORNS O and ZWI JD. The small world of the cerebral cortex. *Neuroinformatics.,* 2: 145-162, 2004.

TZOURIO-MAZOYER N, LANDEAU B, PAPATHANASSIOU D, CRIVELLO F, ETARD O, DELCROIX N, MAZOYER B, and JOLIOT M. Automated anatomical labeling of activations in SPM using a macroscopic anatomical parcellation of the MNI MRI single-subject brain. *Neuroimage.,* 15: 273-289, 2002.

VAN DIJK KR, SABUNCU MR, and BUCKNER RL. The influence of head motion on intrinsic functional connectivity MRI. *Neuroimage.,* 59: 431-438, 2012.

WANG L, LI Y, METZAK P, HE Y, and WOODWARD TS. Age-related changes in topological patterns of large-scale brain functional networks during memory encoding and recognition. *Neuroimage.,* 50: 862-872, 2010.

WECHSLER, D. Wechsler Adult Intelligence Scale—3rd Edition (WAIS-3) San Antonio, TX: Harcourt Assessment, 1997.

WECHSLER, D. Wechsler Abbreviated Scale of Intelligence (WASI). San Antonio, TX: Harcourt Assessment, 1999.

WECHSLER, D. Wechsler Intelligence Scale for Children—4th Edition (WISC-IV). San Antonio, TX: Harcourt Assessment, 2003

ZALESKY A, COCCHI L, FORNITO A, MURRAY MM, and BULLMORE E. Connectivity differences in brain networks. *Neuroimage.,* 60: 1055-1062, 2012.

ZALESKY A, FORNITO A, and BULLMORE E. On the use of correlation as a measure of network connectivity. *Neuroimage.,* 60: 2096-2106, 2012.

Supplemental figures

Fig. S1. Principal component analysis. Analysis was run on the individual main IQs and subtests scores. As a confirm of behavioural data quality, the solution presented in the figure clearly resembles the expected factorial structure of the WASI, showing a three factors solution which segregated FSIQ, PIQ and VIQ, as well their respective subtests. Values on the axis represent factor loadings.

Fig. S2. Between-group comparisons of single pairwise connectivities. The figure shows the Pearson's correlation between all pairwise connectivities (n=4005, AAL atlas) in High and Low IQ participants. A deviation in the connectivity distribution is evident in the lowest part of the graph (orange ellipsoid), with High-IQ individuals showing stronger pairwise connectivities in the left tail of the distribution with respect to Low-IQ ones. Such difference may be responsible

for both the increased variability observed in the robustness towards TA shown in Fig. 2B, as well for the different sets of regions highly responsible for robustness in High and Low-IQ subjects.

Fig.S3. Largest Connected Component drop at the regional level. The distribution of the average *LCC* drop for all the regions in the AAL atlas is shown. Values on the y-axis represents the number of regions being disconnected from the largest connected component after the removal of each region displayed on the x-axis. Brain surfaces show the five lobes and the regions belonging to them.

Fig. S4. Age-related differences. Giving the potential interaction between age, brain robustness and intelligence level, the average LCC size obtained after the complete removal of all nodes (within the individual SW windows) for different age decades has been calculated. Panel A: subjects with higher IQ showed increased robustness levels especially at later ages for both TA and RE (upper and lower row respectively).

Fig. S5. Seed-based connectivity. Regions identified as more responsible for brain robustness drop during TA simulation have been used as seed for pairwise functional connectivity estimation. A comparison between High and Low-IQ participants has been consequently performed (p<.05, FDR corrected). Those regions showing a higher drop in Low-IQ subjects are reported, except for language-related regions which have been included in Fig. 4C. Note: BA6=

superior frontal gyrus; BA8=superior frontal gyrus - medial part; BA11=middle frontal gyrus - pars orbitalis ; BA20=inferior temporal lobe ; BA21= middle temporal lobe; BA23=posterior cingulate cortex.

Fig. S6. Robustness to targeted attacks using different nodal metrics. The panels represent the average size of the *LCC* (*y* axis) during the targeted lesioning procedure, with target nodes being defined using two additional nodal metrics other than *Bc*, that are nodal Degree and Strength. As for the analysis using *Bc*, brain robustness has been computed within the entire sparsity windows, by retaining an increasing percentage of all possible connections in a decreasing-strength fashion, thus ranging from 1% (absolute stronger connections) to 100% (*x* axis). As observed for *Bc*, the results confirm the difference in brain robustness between High and Low IQ participants across the small-worldness sparsity window (~10-30%).

A

BA20   BA21   BA11

BA6   BA8   BA23

High IQ > Low IQ   Low IQ > High IQ   *R*

High vs Low-IQ significant differences

High vs Low-IQ significant differences